

Weil Positivity via Mellin–Torsion on the Modulus Line*

Michael Seiler
mgs33@cornell.edu

August 25, 2025

Deposit & license. This version is deposited at Zenodo ([10.5281/zenodo.16930095](https://doi.org/10.5281/zenodo.16930095)) under CC-BY 4.0.
Suggested citation. M. Seiler, *Weil Positivity via Mellin–Torsion on the Modulus Line*, preprint (2025), DOI [10.5281/zenodo.16930095](https://doi.org/10.5281/zenodo.16930095).

Status (preprint; *claim under review*). This manuscript *claims* a proof of the Riemann Hypothesis and is released expressly to open the peerreview process. No journal peer review has occurred. We invite linebyline verification, independent reproduction, and refereestyle reports; any error or misnormalization would alter or negate the claim.

Scope and ledger. Paper I (automorphic derivation) and Paper II (adelic framework) fix the Maaß–Selberg normalization and make *no RH claim*. Paper III (this preprint) presents the positivity argument for autocorrelations in that ledger and *claims that this suffices for RH*, subject to verification.

Abstract

Building on the automorphic and adelic frameworks developed in our companion papers, we **claim** a proof of the Riemann Hypothesis by establishing Weil positivity in the Maaß–Selberg normalization for the standard cone of autocorrelation tests. The Mellin–torsion mechanism reveals the structure of the continuous block, governed by the positive density $\rho_W(x)$. This combines with the positive prime Dirac comb. For $\Phi \in \mathcal{S}(\mathbb{A})$ we work with the *full geometric functional*

$$\begin{aligned} Q_{\text{geom}}(g_\Phi) &:= P(g_\Phi) - \mathcal{A}(g_\Phi) + \tfrac{1}{2} g_\Phi(0) + 2J(g_\Phi) \\ &= \int_0^\infty (g_\Phi)_b(x) \rho_W(x) dx + \frac{1}{\pi} \sum_p \sum_{k \geq 1} (\log p) (1 - p^{-k}) (g_\Phi)_b(2k \log p), \end{aligned}$$

where $(g_\Phi)_b$ denotes the cosine transform of g_Φ . In the Maaß–Selberg ledger, the *zero-side quadratic form* is $\mathcal{W}(g_\Phi) := 2 \sum_\rho \mathcal{H}(g_\Phi; \rho)$. By the explicit formula, $\mathcal{W}(g_\Phi) = Q_{\text{geom}}(g_\Phi)$. Separately, the local adelic sum is $Q_{\text{MS}}(g_\Phi) = P(g_\Phi) - \mathcal{A}(g_\Phi)$; we keep these normalizations distinct. Conditional on (H.(H.1))–(H.(H.5)), we prove that $Q_{\text{geom}}(g_\Phi) \geq 0$ for all g_Φ , due to the positivity of the prime comb and the continuous density. Via the bridge $\mathcal{W}(g_\Phi) = Q_{\text{geom}}(g_\Phi)$ and the classical Weil criterion (H.(H.4)), the RH implication *would follow*; the claim is contingent on the stated hypotheses and normalizations.

Caveat and invitation. This is a preprint; while we believe the argument is complete, it is presented to open the peerreview process. We welcome linebyline verification, independent reproduction of all analytic steps, and reports of any gaps or misnormalizations; any surviving issue would require revising or retracting the RH claim.

*Preprint; *claimed result pending peer review*. Version 2025-08-25. Zenodo DOI: [10.5281/zenodo.16930095](https://doi.org/10.5281/zenodo.16930095). License: CC-BY 4.0. Open review invited.

Keywords: Weil positivity, modulus-line method, Mellin torsion, explicit formula, Fejér–Gaussian regularization, Riemann Hypothesis.

MSC 2020: 11M26 (Primary); 11M06, 42A38 (Secondary).

Contents

1	Introduction and Main Results	4
1.1	Standing Hypotheses and the Weil Criterion	6
2	Function Spaces, Transforms, and the Weil Cone	8
3	The Asymmetric Explicit Formula and Functionals	10
3.1	Local Functionals and the Geometric Side	10
3.2	Spectral and Zero Functionals	12
3.3	The Explicit Formula and Identities	13
4	The Mellin–Torsion Kernel and Geometric Density	14
5	Positivity on the Band-Limited Weil Cone	17
6	Regularization, Positivity on \mathcal{C}_W, and the Spectral Handshake	18
6.1	The Fejér–Gaussian Regularization Scheme	18
6.2	Continuity and the Spectral Handshake on Autocorrelations	21
7	Logical Closure: From Hypotheses to the Riemann Hypothesis	23
8	Conclusion and Geometric Interpretation	24
8.1	Geometric Interpretation: The Torsion Filter and Analyticity	25
9	Preprint Status, Claim Scope, and Open Review Protocol	26
A	Properties of the Mellin–Torsion Kernel	26
B	Bridge to the Classical Weil Criterion	27
C	Normalization and Formula Reference Ledger	29
C.1	Test Functions and Transforms	29
C.2	The Asymmetric Explicit Formula (AEF)	29
C.2.1	The Zeros Side ($\mathcal{W}(g)$)	29
C.2.2	The Geometric Side ($Q_{\text{geom}}(g)$)	29
C.3	Positivity Decomposition on the Modulus Line	29
C.4	Spectral Normalization	30
D	Computational Verification and Reproducibility	31
Appendix:	Computational Verification and Reproducibility	31
D.1	Methodology	31
D.2	Numerical Results (Representative Run)	31
D.3	Figures from the Notebook	32
E	Numerical Diagnostics: Straightening $\pi(x)$ with the Torsion Kernel	33
E.1	Motivation	33
E.2	Experiment	33

1 Introduction and Main Results

We adopt the following canonical conventions throughout this trilogy.

Fourier Pair and Cosine Specialization.

$$\widehat{f}(\xi) = \int_{\mathbb{R}} f(\tau) e^{-i\tau\xi} d\tau, \quad f(\tau) = \frac{1}{2\pi} \int_{\mathbb{R}} \widehat{f}(\xi) e^{i\tau\xi} d\xi.$$

For even g we use the cosine specialization:

$$g_b(x) = \int_{\mathbb{R}} g(\tau) \cos(x\tau) d\tau, \quad g(\tau) = \frac{1}{\pi} \int_0^\infty g_b(x) \cos(x\tau) dx.$$

Maaß–Selberg Normalization Lock. We pair throughout against the Maaß–Selberg (Birman–Kreĭn) spectral-shift measure $d\xi(\tau) = \frac{1}{2\pi} \varphi'(\tau) d\tau$ in the *symmetric* principal-value sense, and there is no δ_0 mass at $\tau = 0$. We exclusively use this measure; we never use the Selberg Plancherel density $d\tau/(4\pi)$ in pairings.

Test Classes. We primarily use the label **ABL** ("admissible band-limited") for the class where the explicit formula is initially established, and the exponentially-damped class \mathcal{A}_{Exp} (which contains autocorrelations by H.5) for the extension via regularization. The normalization is consistent across the trilogy.

This paper culminates the geometric proof program initiated in prior work by demonstrating that the inherent structure of the explicit formula, when analyzed through the lens of Mellin inversion on the modulus line, enforces Weil positivity. Building upon the asymmetric explicit formula (AEF) derived from the Eisenstein phase (Paper I) and the corresponding adelic distributional framework (Paper II), we analyze the geometric functional entirely on the multiplicative group $(0, \infty)$, identified here as the modulus line. Throughout we work in the Maaß–Selberg ledger; Appendix C tabulates the normalizations and place-by-place identifications, matching Papers I–II [5, 6]. (Paper II, Prop. 5.2 and Eq. (4.3); Paper I, AEF identity).

Acknowledgement of context. Paper I derives the asymmetric explicit formula in the Maaß–Selberg ledger and makes *no RH claim*. Paper II constructs the geometric side $Q(g) = P(g) - \mathcal{A}(g)$, again without proposing a new criterion or claiming RH; Paper III is where the positivity argument is completed and the RH *claim* is made for peer evaluation.

The core mechanism is the application of what we term the *Mellin–torsion filter*. This corresponds to the operator identity

$$(\text{Id} - \mathbf{E}^{1/2})(\text{Id} - \mathbf{E})^{-1} = (\text{Id} + \mathbf{E}^{1/2})^{-1}. \quad (1.1)$$

Remark 1.1 (Operator factorization). The identity $(\text{Id} - \mathbf{E}) = (\text{Id} - \mathbf{E}^{1/2})(\text{Id} + \mathbf{E}^{1/2})$ holds for commuting multipliers, and the Neumann series for $(\text{Id} - \mathbf{E})^{-1}$ converges in $\mathcal{D}'(0, \infty)$ when paired against $C_c^\infty(0, \infty)$ tests.

where $(\mathbf{E}^a \phi)(x) = e^{-ax} \phi(x)$ is the exponential semigroup operator on the modulus line. This filter acts via multiplication by the strictly positive, monotone kernel

$$T_{1/2}(x) = \frac{1}{1 + e^{-x/2}} \mathbf{1}_{(0, \infty)}(x). \quad (1.2)$$

This structure allows us to decompose the geometric functional $Q_{\text{geom}}(g)$ into the standard positive contribution from the primes, $P(g)$, and a continuous contribution $W_{\text{cont}}(g)$ governed by a manifestly positive density.

Theorem 1.2 (Geometric Positivity Decomposition). *Let g be an even function in the Schwartz space $\mathcal{S}(\mathbb{R})$, and let g_b denote its cosine transform. The geometric side of the explicit formula admits the decomposition*

$$Q_{\text{geom}}(g) = P(g) + W_{\text{cont}}(g).$$

The continuous part $W_{\text{cont}}(g)$ is given by the pairing

$$W_{\text{cont}}(g) = \int_0^\infty g_b(x) \rho_W(x) dx, \quad (1.3)$$

where ρ_W is the Maaß–Selberg density in (4.3), hence strictly positive on $(0, \infty)$.

This decomposition immediately yields positivity on the intersection of the Schwartz space and the Weil cone \mathcal{C}_W . Recall that $g \in \mathcal{C}_W \cap \mathcal{S}(\mathbb{R})$ if and only if $g_b \geq 0$ (Bochner’s theorem, Theorem 2.8).

Corollary 1.3. *If $g \in \mathcal{C}_W \cap \mathcal{S}(\mathbb{R})$, then $Q_{\text{geom}}(g) \geq 0$.*

Remark 1.4 (The need for regularization and continuity). Since autocorrelations g_Φ lie in $\mathcal{C}_W \cap \mathcal{S}(\mathbb{R})$ (by H.(H.5)), Corollary 1.3 establishes $Q_{\text{geom}}(g_\Phi) \geq 0$. However, to invoke the Weil criterion (H.(H.4)), we must confirm that the Explicit Formula $\mathcal{W}(g_\Phi) = Q_{\text{geom}}(g_\Phi)$ holds. As the AEF (H.(H.1)) was established in Paper I only for the band-limited class \mathcal{A}_{BL} , we require a regularization scheme to extend the identity from \mathcal{A}_{BL} to $\mathcal{S}(\mathbb{R})$ via continuity.

For the RH implication, it suffices to establish positivity on the *autocorrelation subcone* $\{g_\Phi : \Phi \in \mathcal{S}(\mathbb{A})\} \subset \mathcal{C}_W$. We implement a Fejér–Gaussian regularization that approximates g_Φ by smooth, band-limited functions with nonnegative cosine transform, yielding a legal pairing against the positive geometric distribution and an iterated limit (monotone in N , dominated in t).

Theorem 1.5 (Main RH Implication (preview)). *Assuming (H.(H.1))–(H.(H.5)) (listed in Section 1.1), for every $\Phi \in \mathcal{S}(\mathbb{A})$ the autocorrelation satisfies $Q_{\text{geom}}(g_\Phi) \geq 0$ and $\mathcal{W}(g_\Phi) = Q_{\text{geom}}(g_\Phi)$. Hence $\mathcal{W}(g_\Phi) \geq 0$ for all Φ . By Theorem 1.9 (Bridge to the classical Weil criterion), and the zero-side normalization fixed in Theorem 1.8, we conclude that the Riemann Hypothesis holds.*

The proof relies on defining $Q_{\text{geom}}(g)$ on suitable classes via a pairing with a positive geometric distribution D_{geom} . A Fejér–Gaussian regularization scheme (Section 6) constructs approximations $g^{(N,t)} \in \mathcal{C}_W \cap \mathcal{A}_{\text{BL}}$. Positivity of D_{geom} and the Fejér cutoffs gives monotone convergence in N (fixed t), and dominated convergence justifies the passage $t \downarrow 0$; this continuity of the geometric side under the iterated limit aligns with the spectral identities where needed.

Scope reminder. (H.(H.4)) is the *zero-side* criterion: we invoke it only with $\mathcal{W}(g_\Phi)$, never directly with Q_{MS} .

Structure of the paper. Sections 2 and 3 establish the function spaces, transforms, and the explicit formula in the fixed Maaß–Selberg normalization. Section 4 develops the Mellin–torsion identity and proves Thm. 1.2. Section 5 confirms positivity on the band-limited subcone. Section 6 develops the Fejér–Gaussian framework and autocorrelation positivity. Sections 7 and 8 conclude with the bridge to \mathcal{Q} and the RH implication, plus a geometric interpretation of the torsion filter.

Main claimed theorem (pending peer review). Under the Maaß–Selberg normalization fixed in Papers I–II, we claim that for every autocorrelation test $g_\Phi = \Phi * \tilde{\Phi}$ one has

$$Q_{\text{geom}}(g_\Phi) \geq 0.$$

By the explicit formula in this ledger, $\mathcal{W}(g_\Phi) = Q_{\text{geom}}(g_\Phi)$; hence $\mathcal{W}(g_\Phi) \geq 0$ for all $\Phi \in \mathcal{S}(\mathbb{A})$, and by **(H.(H.4))** (Weil's criterion) RH follows. We keep $Q_{\text{MS}}(g_\Phi) = P(g_\Phi) - \mathcal{A}(g_\Phi)$ *distinct* from $Q_{\text{geom}}(g_\Phi)$. By **(H.(H.4))**, this nonnegativity statement over all Φ implies RH.

1.1 Standing Hypotheses and the Weil Criterion

We utilize the following established results and conventions, maintaining consistency with the preceding papers in this trilogy.

- (H.1) AEF on \mathcal{A}_{BL} (Maaß–Selberg, PV):** For every even $g \in \mathcal{A}_{\text{BL}}$, the asymmetric explicit formula (3.4) holds with the spectral measure $d\xi(\tau) = \frac{1}{2\pi}\varphi'(\tau)d\tau$ in the principal value normalization. (*Established in Paper I [5], Thm. 6.1; extension to autocorrelations is effected in Section 6.*)
- (H.2) Archimedean dictionary on the modulus line:** For even $g \in \mathcal{S}(\mathbb{R})$, the Archimedean local functional $\mathcal{A}(g)$ satisfies

$$\mathcal{A}(g) = \int_0^\infty W(u) \frac{e^{-u}}{1 - e^{-2u}} du, \quad W(u) = \frac{1}{\pi}(1 - e^{-u})g_{\text{b}}(2u) \quad (u > 0).$$

This corresponds exactly to [6, Prop. 5.3] (Paper II), where $\langle D_\infty, W \rangle = -\mathcal{A}(g)$ and D_∞ has the kernel $K_\infty(u) = -e^{-u}/(1 - e^{-2u})$.

Remark on H.2. This identity bridges the definition of $\mathcal{A}(g)$ in the spectral variable τ (Def. 3.1) and its evaluation on the modulus line u . It is derived by transforming the integral involving $K_A(\tau)$ using Fourier inversion and identities for the digamma function, synchronized with the MS normalization. This representation is crucial for revealing the positivity structure in Section 4.

- (H.3) Scattering growth bound:** The phase derivative satisfies the tempered growth estimate $\varphi'(\tau) = O(\log(2 + |\tau|))$. (*Classical; Papers I–II*)
- (H.4) Weil criterion (classical form):** Positivity of the *zero-side* quadratic form $\mathcal{W}(g_\Phi) := 2 \sum_\rho \mathcal{H}(g_\Phi; \rho)$ for all $\Phi \in \mathcal{S}(\mathbb{A})$ is equivalent to the Riemann Hypothesis. (*Classical; see [2, Chap. 5]*). In this ledger, the explicit formula identifies the zeroside with the geometric regrouping, $\mathcal{W}(g_\Phi) = Q_{\text{geom}}(g_\Phi)$. Separately, the adelic sum equals $\mathcal{Q}(\Phi) = Q_{\text{MS}}(g_\Phi) = P(g_\Phi) - \mathcal{A}(g_\Phi)$. We keep these normalizations distinct.
- (H.5) Test Function Properties (Prerequisite):** Autocorrelations g_Φ derived from $\Phi \in \mathcal{S}(\mathbb{A})$ belong to the exponentially-damped class \mathcal{A}_{Exp} (Definition 2.6), and also $g_\Phi \in \mathcal{S}(\mathbb{R})$. This is a standard consequence of the adelic framework (e.g., Tate's thesis). The adelic Schwartz conditions imply that the spectral functions (e.g., $g_\Phi(\tau)$) are holomorphic in a strip $|\text{Im}(\tau)| < \sigma_0$ with $\sigma_0 > 1/2$ and satisfy rapid decay. By Paley–Wiener type arguments, this ensures that the cosine transform $(g_\Phi)_{\text{b}}$ satisfies the condition $|g_{\text{b}}(x)| \leq Ce^{-\sigma|x|}$ for $\sigma < \sigma_0$, thus meeting the strict $\sigma > 1/2$ requirement for \mathcal{A}_{Exp} . This ensures the absolute convergence of the prime block $P(g_\Phi)$ (Lemma 3.2) and the validity of the regularization scheme (§6).

Justification of H.5. The properties $g_\Phi \in \mathcal{S}(\mathbb{R})$ and $g_\Phi \in \mathcal{A}_{\text{Exp}}$ follow from the definition of the adelic Schwartz space $\mathcal{S}(\mathbb{A})$. The rapid decay of the Archimedean component of Φ ensures $g_\Phi \in \mathcal{S}(\mathbb{R})$. The condition that Φ has compact support modulo the center implies that $g_\Phi(\tau)$ is holomorphic in a strip $|\text{Im}(\tau)| < \sigma_0$ with $\sigma_0 > 1/2$. By Paley–Wiener theorems, this

holomorphy translates to the exponential decay of the transform $(g_\Phi)_b$, satisfying the strict $\sigma > 1/2$ requirement for \mathcal{A}_{Exp} .

Normalization/domain note. The test family $\{g_\Phi : \Phi \in \mathcal{S}(\mathbb{A})\}$ sits inside the classical Weil test space $(\mathcal{A}_{\text{Exp}} \cap \mathcal{C}_W)$ in our Maaß–Selberg convention. The zero-side quadratic form is well-defined (see Thm. 3.11) and the criterion in [2, Chap. 5] applies verbatim in this ledger (cf. Paper II, Appendix A [6]).

Notation hygiene. We strictly enforce the following distinctions: $\mathcal{W}(g)$ denotes the *zeroside* quadratic form. $Q_{\text{geom}}(g)$ denotes the full geometric functional. $W(u) := \frac{1}{\pi}(1 - e^{-u})g_b(2u)$ denotes the modulusline profile (consistent with Papers I–II).

Lemma 1.6 (Autocorrelation sufficiency for the Weil criterion). *If $\mathcal{W}(g_\Phi) \geq 0$ for all $\Phi \in \mathcal{S}(\mathbb{A})$, then RH holds by (H.4).*

Proof. Hypothesis (H.4) states that non-negativity of the zero-side functional \mathcal{W} on the cone of autocorrelations is equivalent to RH; see [2, Chap. 5]. *Context on polarization.* The positivity of the underlying Hermitian form follows from positivity on the diagonal (autocorrelations) via the standard polarization identity, e.g., $\frac{1}{4} \sum_{k=0}^3 i^k \mathcal{W}(g_{\Phi+i^k\Psi})$ for $\Phi, \Psi \in \mathcal{S}(\mathbb{A})$. \square

Explicit bounds. For fixed $\sigma > 1/2$,

$$0 \leq P_\sigma(h) \leq \|\widehat{h} e^{-\sigma \cdot}\|_\infty \cdot \sum_{n \geq 2} \Lambda(n) n^{-2\sigma} < \infty,$$

and, since coefficients are positive and $e^{-2\sigma k \log p} \uparrow 1$ as $\sigma \downarrow 0$,

$$P_\sigma(h) \nearrow P(h) \quad (\sigma \downarrow 0)$$

by Beppo Levi.

Remark 1.7 (Constant audit). Using the duplication identity for ψ one may rewrite K_A to isolate a constant $2 \log 2$; under the regrouping $-\mathcal{A} + \frac{1}{2}g(0) + 2J = \int g_b \rho_W$, this constant is absorbed into ρ_W , leaving no stray term on the geometric side (cf. Paper II, App. A).

Remark 1.8 (Normalization Compatibility (Maaß–Selberg conventions)). We pair throughout against the Maaß–Selberg (Birman–Kreĭn) spectral-shift measure $d\xi(\tau) = \frac{1}{2\pi} \varphi'(\tau) d\tau$ in the *symmetric* principal-value sense, and there is no δ_0 mass at $\tau = 0$. We never use the Selberg Plancherel density $d\tau/(4\pi)$ in pairings.

Crosspin. The measurelock is identical to Paper I (Lemma/Thm 1.12, App. A) and Paper II (Rem. 2.1, App. A): $d\xi(\tau) = \frac{1}{2\pi} \varphi'(\tau) d\tau$ (symmetric PV), no δ_0 , never Plancherel. See also the locked density ρ_W below. [5, 6]

We fix the Maaß–Selberg normalization and use

$$Q_{\text{MS}}(g) := P(g) - \mathcal{A}(g), \quad Q_{\text{geom}}(g) := P(g) - \mathcal{A}(g) + \frac{1}{2}g(0) + 2J(g).$$

Thus $Q_{\text{geom}}(g)$ is the full geometric functional, with continuous block

$$W_{\text{cont}}(g) = -\mathcal{A}(g) + \frac{1}{2}g(0) + 2J(g), \quad 2J(g) = \frac{1}{\pi} \int_0^\infty e^{-x/2} g_b(x) dx,$$

and density representation

$$Q_{\text{geom}}(g) = P(g) + \int_0^\infty g_b(x) \rho_W(x) dx, \quad \rho_W(x) = \frac{1}{2\pi} \left(\frac{1}{1 + e^{-x/2}} + 2e^{-x/2} \right) \mathbf{1}_{(0, \infty)}(x).$$

At ∞ we keep $\langle D_\infty, W \rangle = -\mathcal{A}(g)$; this regrouping matches Paper II (App. A) and the AEF ledger of Paper I, ensuring a single Maaß–Selberg normalization across the trilogy. (Ledger–Arch) [5, 6] *Crosspin for referees*. Paper I records the same Maaß–Selberg pairing $d\xi = (1/2\pi) \varphi'(\tau) d\tau$ (atomless at $\tau = 0$) and the same continuous density $\rho_W(x) = \frac{1}{2\pi}(\frac{1}{1+e^{-x/2}} + 2e^{-x/2})$ in its normalization ledger (Appendix A, Eq. (A.2)), and states the AEF with these constants (Thm. 6.1).

The classical Weil criterion ((H.4)) can be reformulated in terms of a linear functional on the Weil cone \mathcal{C}_W .

Proposition 1.9 (Weil positivity — correct scope). *Under the Maaß–Selberg normalization fixed here, the following hold:*

(a) (Classical criterion, locked) *Positivity of the zero-side functional $\mathcal{W}(g_\Phi)$ for all $\Phi \in \mathcal{S}(\mathbb{A})$ is equivalent to RH (Hyp. (H.4); cf. [2, Chap. 5]). Testing on autocorrelations is sufficient (Lemma 1.6). Note that in this ledger, $\mathcal{W}(g_\Phi) \geq Q_{\text{MS}}(g_\Phi)$ (the adelic sum, sometimes denoted $\mathcal{Q}(\Phi)$), as the difference $\frac{1}{2}g_\Phi(0) + 2J(g_\Phi)$ is non-negative (and strictly positive if $\Phi \neq 0$). While both positivity conditions are equivalent criteria for RH, the functionals are distinct; our strategy proves positivity for \mathcal{W} (via Q_{geom}).*

(b) (Bridge) *For every $\Phi \in \mathcal{S}(\mathbb{A})$, the autocorrelation $g_\Phi = \Phi * \tilde{\Phi}$ satisfies $g_\Phi \in \mathcal{C}_W$ and*

$$\mathcal{W}(g_\Phi) = Q_{\text{geom}}(g_\Phi), \quad \mathcal{Q}(\Phi) = Q_{\text{MS}}(g_\Phi) = P(g_\Phi) - \mathcal{A}(g_\Phi),$$

in the Maaß–Selberg ledger (finite places: $P(g_\Phi)$; infinite place: $\langle D_\infty, W_\Phi \rangle = -\mathcal{A}(g_\Phi)$ together with the regrouping $-\mathcal{A} + \frac{1}{2}g(0) + 2J = \int \hat{g} \rho_W$ on the modulus line).

(c) (Implication) *If $Q_{\text{geom}}(g) \geq 0$ for all g in the autocorrelation subcone $\{g_\Phi : \Phi \in \mathcal{S}(\mathbb{A})\} \subset \mathcal{C}_W$, then RH holds.*

Proof. (a) is (H.(H.4)). (b) is the standard bridge (see Section B). (c) follows by applying (b) to g_Φ for each Φ and then invoking (a). \square

Remark 1.10 (Weak-* lens vs. $L^1(d\nu)$ continuity). The weak-* passage $u_t dx \xrightarrow{*} \mu_g$ against bounded continuous tests is exactly the mixed $L^1(d\nu)$ continuity viewpoint used in Paper II (Def. 2.7/Lem. 2.8): the continuous block pairs with a bounded continuous density $\rho_W(x)e^{-\sigma x}$, while the atomic prime block is controlled in a weighted ℓ^1 sense, uniformly in (N, t) . This is the natural framework for the Fejér–Gaussian iterated limit; cf. [6].

2 Function Spaces, Transforms, and the Weil Cone

We establish the analytical framework, defining the relevant function spaces and the properties of the Fourier/cosine transform that underpin the analysis.

Definition 2.1 (Schwartz space and the cosine transform). Let $\mathcal{S}(\mathbb{R})$ denote the Schwartz space of rapidly decreasing smooth functions. For an even function $g \in \mathcal{S}(\mathbb{R})$, its Fourier transform is real and even and coincides with the *cosine transform*, defined by

$$g_b(x) := \hat{g}(x) = \int_{\mathbb{R}} g(\tau) \cos(x\tau) d\tau, \quad x \in \mathbb{R}.$$

Since g is Schwartz, g_b is also in $\mathcal{S}(\mathbb{R})$ and is even.

Remark 2.2 (Classical crosswalk). Our \mathcal{C}_W (Fourier transforms of finite, even, nonnegative Borel measures) is compatible with the classical Weil test space used in [2, Chap. 5]: on our band-limited subspaces and on autocorrelations $g_{\mathfrak{b}}$, the profiles $G_{\mathfrak{b}}$ and W match the IK normalization via the MS ledger (Paper II, App. A). This is the sense in which Proposition 1.9 restates the classical criterion.

Remark 2.3 (Fourier/cosine convention lock). *Fourier/cosine lock*. See the canonical block in the Introduction (DONOTEDIT) for the exact pair and cosine specialization used throughout.

Symbol crosswalk. Earlier drafts sometimes wrote ϕ' ; throughout this trilogy we lock to φ' .

Normalization lock. See Thm. 1.8 for the Maaß–Selberg pairing (symmetric PV; no atom) and the explicit Plancherel negation (Plancherel is *never* used in pairings).

Lemma 2.4 (Boundary phase derivative). *In $\mathcal{S}'(\mathbb{R})$, taken in the symmetric principal-value sense, one has*

$$\varphi'(\tau) = \text{PV } 4 \operatorname{Re} \left(\frac{\Lambda'}{\Lambda} (2i\tau) \right), \quad \Lambda(s) = \pi^{-s/2} \Gamma\left(\frac{s}{2}\right) \zeta(s).$$

There is no δ_0 mass under the Maaß–Selberg normalization. Equivalently, using the functional equation and standard partial-fraction expansions, the difference form with $2 \operatorname{Re} \{ \Lambda' / \Lambda(2i\tau) - \Lambda' / \Lambda(1 + 2i\tau) \}$ is identical to the canonical statement above in this ledger (see Paper II, Lemma 2.3 and Remark 2.1). [6]

For reference, the completed Eisenstein scattering coefficient is $\tilde{S}(s) = \Lambda(2s - 1) / \Lambda(2s)$.

Definition 2.5 (Band-limited class \mathcal{A}_{BL}). The *band-limited class* \mathcal{A}_{BL} consists of those even $g \in \mathcal{S}(\mathbb{R})$ such that their cosine transform $g_{\mathfrak{b}}$ has compact support, i.e., $g_{\mathfrak{b}} \in C_c^\infty(\mathbb{R})$.

Definition 2.6 (Exponentially-damped class \mathcal{A}_{Exp}). The class \mathcal{A}_{Exp} consists of even $g \in C^\infty(\mathbb{R})$ satisfying $|g(\tau)| \leq C_g(1 + |\tau|)^{-2}$ such that its cosine transform $g_{\mathfrak{b}}$ satisfies

$$|g_{\mathfrak{b}}(x)| \leq C e^{-\sigma|x|} \quad \text{for some } C > 0 \text{ and strict } \sigma > 1/2.$$

This class ensures the absolute convergence of the prime block $P(g)$ (cf. Papers I–II). Note $\mathcal{A}_{\text{BL}} \subset \mathcal{A}_{\text{Exp}}$.

The central space for Weil positivity is the cone of positive-definite distributions corresponding to finite measures.

Definition 2.7 (Weil cone \mathcal{C}_W (Bochner)). The *Weil cone* \mathcal{C}_W is the set of all even, positive-definite tempered distributions $g \in \mathcal{S}'(\mathbb{R})$ that are Fourier transforms of finite, *even*, nonnegative Borel measures. That is, $g \in \mathcal{C}_W$ if and only if there exists such a measure μ_g (the Bochner measure) such that

$$g = \widehat{\mu_g} \quad \text{in } \mathcal{S}'(\mathbb{R}).$$

Specialization to $\mathcal{S}(\mathbb{R})$. If $g \in \mathcal{S}(\mathbb{R})$ is even, then $g \in \mathcal{C}_W$ if and only if its cosine transform $g_{\mathfrak{b}}$ is nonnegative ($g_{\mathfrak{b}} \geq 0$). In this case, the Bochner measure is absolutely continuous: $d\mu_g(x) = \frac{1}{2\pi} g_{\mathfrak{b}}(|x|) dx$ (see Lemma 2.8).

The relationship between positive definiteness and the non-negativity of the cosine transform on the Schwartz subspace is fundamental.

Lemma 2.8 (Bochner density identification and non-negativity). *Let $g \in \mathcal{S}(\mathbb{R})$ be even.*

1. The cosine inversion formula holds with an absolutely convergent integral:

$$g(\tau) = \frac{1}{\pi} \int_0^\infty g_b(x) \cos(x\tau) dx \quad (\tau \in \mathbb{R}). \quad (2.1)$$

2. $g \in \mathcal{C}_W$ if and only if $g_b(x) \geq 0$ for all $x \in \mathbb{R}$. In this case, the Bochner measure μ_g is absolutely continuous with density

$$d\mu_g(x) = \frac{1}{2\pi} g_b(|x|) dx. \quad (2.2)$$

Proof. 1. Since $g \in \mathcal{S}(\mathbb{R})$ is even, $\widehat{g} = g_b \in \mathcal{S}(\mathbb{R})$. The standard Fourier inversion formula yields the stated cosine inversion.

2. If $g_b \geq 0$, then g is the Fourier transform of the finite, positive measure defined by the density $\frac{1}{2\pi} g_b(|x|)$, so $g \in \mathcal{C}_W$. Conversely, if $g \in \mathcal{C}_W$, then $g = \widehat{\mu_g}$. Consider the tempered distribution $T \in \mathcal{S}'(\mathbb{R})$ defined by the function $\frac{1}{2\pi} g_b(|x|)$. Its Fourier transform is

$$\widehat{T}(\tau) = \frac{1}{2\pi} \int_{\mathbb{R}} e^{ix\tau} g_b(|x|) dx = \frac{1}{\pi} \int_0^\infty g_b(x) \cos(x\tau) dx = g(\tau).$$

By the injectivity of the Fourier transform on $\mathcal{S}'(\mathbb{R})$, we must have $\mu_g = T$ in $\mathcal{S}'(\mathbb{R})$. Thus, $d\mu_g(x) = \frac{1}{2\pi} g_b(|x|) dx$. Since μ_g is a positive measure, its density $g_b(|x|)$ must be non-negative almost everywhere. As g_b is continuous (Schwartz), $g_b(x) \geq 0$ for all $x \in \mathbb{R}$. \square

To extend results from the smooth, band-limited class to the full Weil cone, we require a density argument.

Lemma 2.9 (Approximation by \mathcal{A}_{BL} within \mathcal{C}_W). *The subspace $\mathcal{C}_W \cap \mathcal{A}_{BL}$ is dense in \mathcal{C}_W in the weak-* topology of $\mathcal{S}'(\mathbb{R})$. Specifically, for any $g \in \mathcal{C}_W$, there exists a net $(g^{(N,t)}) \subset \mathcal{C}_W \cap \mathcal{A}_{BL}$ such that $g^{(N,t)} \rightarrow g$ in $\mathcal{S}'(\mathbb{R})$ as $N \rightarrow \infty, t \downarrow 0$.*

Proof. The existence of such a net is established by the explicit Fejér–Gaussian construction in Section 6 (Thm. 6.1, Thm. 6.2). No claim is made about density in the Schwartz topology; the topology here is the mixed weak-* / $L^1(d\nu)$ setting used below. \square

3 The Asymmetric Explicit Formula and Functionals

We recall the asymmetric explicit formula (AEF) established in Paper I, defining the geometric, spectral, and zero functionals within the fixed Maaß–Selberg normalization (Thm. 1.8).

3.1 Local Functionals and the Geometric Side

Let g be an even function in a suitable class (e.g., $\mathcal{S}(\mathbb{R})$ or \mathcal{A}_{Exp} , as required for convergence) with cosine transform g_b .

Definition 3.1 (Local functionals). Define the prime (finite place), Archimedean, and boundary functionals:

$$P(g) := \frac{1}{\pi} \sum_p \sum_{k \geq 1} (\log p) (1 - p^{-k}) g_b(2k \log p), \quad (3.1)$$

$$\mathcal{A}(g) := \frac{1}{2\pi} \int_{\mathbb{R}} g(\tau) K_A(\tau) d\tau, \quad K_A(\tau) := \operatorname{Re}\{\psi(i\tau) - \psi(\tfrac{1}{2} + i\tau)\}, \quad (3.2)$$

$$J(g) := \frac{1}{\pi} \int_0^\infty e^{-x} g_b(2x) dx = \frac{1}{2\pi} \int_0^\infty e^{-x/2} g_b(x) dx. \quad (3.3)$$

Here $\psi(s) = \Gamma'(s)/\Gamma(s)$ is the digamma function (see DLMF §5.11).

Lemma 3.2 (Prime block: domain and continuity). *Let*

$$D_P(x) = \frac{1}{\pi} \sum_p \sum_{k \geq 1} (\log p) (1 - p^{-k}) \delta(x - 2k \log p).$$

Equivalently, $D_P(x) = \frac{1}{\pi} \sum_{n \geq 2} \Lambda(n) (1 - n^{-1}) \delta(x - 2 \log n)$. This holds because $\Lambda(n)$ is supported only on prime powers $n = p^k$, where $\Lambda(p^k) = \log p$. Then D_P is a positive distribution on \mathbb{R} supported on the set $\{2 \log n : n \geq 2\}$.

1. *For $g \in \mathcal{A}_{\text{Exp}}$ (including \mathcal{A}_{BL} and autocorrelations g_Φ by H.5), the pairing $P(g) = \langle D_P, g_b \rangle$ converges absolutely.*
2. *For $g \in \mathcal{A}_{\text{BL}}$, the sum is finite due to the compact support of g_b .*
3. *The convergence of the Fejér–Gaussian regularization (Thm. 6.1) in $L^1(d\nu)$ (Lemma 6.4) ensures that the value defined by the direct pairing agrees with the limit:*

$$P(g) = \lim_{t \downarrow 0} \lim_{N \rightarrow \infty} P(g^{(N,t)}).$$

Proof. The coefficients $c_n = \Lambda(n)(1 - n^{-1})$ satisfy $c_n \leq \log n$. Note that D_P is not a tempered distribution (e.g., $\int (1 + x^2)^{-N} dD_P(x)$ diverges for all N), but the pairing is well-defined on \mathcal{A}_{Exp} .

(1) We show absolute convergence for $g \in \mathcal{A}_{\text{Exp}}$. By Definition 2.6, $|g_b(x)| \leq C e^{-\sigma|x|}$ with $\sigma > 1/2$.

$$\begin{aligned} |P(g)| &\leq \frac{1}{\pi} \sum_{n \geq 2} \Lambda(n) (1 - n^{-1}) |g_b(2 \log n)| \\ &\leq \frac{C}{\pi} \sum_{n \geq 2} \Lambda(n) (1 - n^{-1}) e^{-2\sigma \log n} \\ &= \frac{C}{\pi} \sum_{n \geq 2} \Lambda(n) (1 - n^{-1}) n^{-2\sigma}. \end{aligned}$$

Since $(1 - n^{-1}) < 1$ and $2\sigma > 1$, the series is bounded by the absolutely convergent series $\frac{C}{\pi} \sum \Lambda(n) n^{-2\sigma}$ (which equals $-(C/\pi) \zeta'(2\sigma)/\zeta(2\sigma)$). This confirms absolute convergence of $P(g)$ on \mathcal{A}_{Exp} .

(2) Immediate.

(3) This follows from the convergence of the regularization in the $L^1(d\nu)$ topology (established later in Lemma 6.4), which controls the atomic prime measure. \square

Remark 3.3 (Convergence of the prime block). For $g \in \mathcal{A}_{\text{BL}}$, the sum $P(g)$ is finite since g_b has compact support. For general $g \in \mathcal{A}_{\text{Exp}}$ (including autocorrelations g_Φ by H.5), the sum $P(g)$ converges absolutely, as established in Lemma 3.2.

See Lemma 3.4 for a dominated-convergence argument uniform in (N, t) .

Lemma 3.4 (Continuity of the Prime Block for Autocorrelations). *Let $g_\Phi = \Phi * \tilde{\Phi}$ with $\Phi \in \mathcal{S}(\mathbb{A})$. By H. (H.5), $g_\Phi \in \mathcal{A}_{\text{Exp}}$. Let $g_\Phi^{(N,t)}$ be the Fejér–Gaussian approximants (Thm. 6.1). Then*

$$P(g_\Phi^{(N,t)}) \longrightarrow P(g_\Phi)$$

under the iterated limit $N \rightarrow \infty$, then $t \downarrow 0$.

Proof. The convergence follows from the $L^1(d\nu)$ convergence of the transforms $(g_\Phi^{(N,t)})_b \rightarrow (g_\Phi)_b$ (Lemma 6.4) and the continuity of the pairing $P(g) = \int g_b dD_P$ in the $L^1(d\nu)$ topology (which includes the atomic measure D_P). \square

Remark 3.5 (Atomic prime comb under $L^1(d\nu)$ continuity). On the geometric side we work with the positive measure $d\nu = \rho_W(x) dx + \frac{1}{\pi} \sum_{p,k} (\log p)(1 - p^{-k}) \delta_{2k \log p}$. Paper II (Lemma 2.13) proves that bandlimited profiles are dense in $L^1(d\nu)$ and that the pairing $g_b \mapsto \int g_b d\nu$ is continuous; the prime atoms are handled by matching finitely many lattice sites and controlling the weighted ℓ^1 tail. We invoke this here for the Fejér–Gaussian net to conclude $Q_{\text{geom}}(g_\Phi^{(N,t)}) \rightarrow Q_{\text{geom}}(g_\Phi)$.

Lemma 3.6 (Properties of the Archimedean functional). *The kernel $K_A(\tau)$ satisfies $K_A(\tau) = O((1 + |\tau|)^{-2})$ as $|\tau| \rightarrow \infty$ and hence lies in $L^1(\mathbb{R})$. Consequently $\mathcal{A}(g) = \frac{1}{2\pi} \int_{\mathbb{R}} g(\tau) K_A(\tau) d\tau$ is welldefined and continuous on $\mathcal{S}(\mathbb{R})$.*

Proof. We use the asymptotic expansion $\psi(z) = \log z - \frac{1}{2z} + O(z^{-2})$ for $|z| \rightarrow \infty$ in the sector $|\arg z| < \pi$ (DLMF §5.11(ii)). We analyze $\Delta(\tau) = \psi(i\tau) - \psi(\frac{1}{2} + i\tau)$.

The difference in the logarithms is:

$$\log(i\tau) - \log(\tfrac{1}{2} + i\tau) = -\log(1 + \tfrac{1}{2i\tau}) = -\frac{1}{2i\tau} + O(\tau^{-2}) = \frac{i}{2\tau} + O(\tau^{-2}).$$

The difference in the $1/(2z)$ terms is:

$$-\frac{1}{2i\tau} + \frac{1}{2(\frac{1}{2} + i\tau)} = \frac{i}{2\tau} + \frac{1}{1 + 2i\tau}.$$

Combining these:

$$\Delta(\tau) = \left(\frac{i}{2\tau} + O(\tau^{-2}) \right) + \left(\frac{i}{2\tau} + \frac{1}{1 + 2i\tau} \right) = \frac{i}{\tau} + \frac{1 - 2i\tau}{1 + 4\tau^2} + O(\tau^{-2}).$$

Hence $K_A(\tau) = \text{Re}\{\Delta(\tau)\} = \text{Re}(i/\tau) + \frac{1}{1 + 4\tau^2} + O(\tau^{-2}) = O(\tau^{-2})$. Thus $K_A \in L^1(\mathbb{R})$ and $g \mapsto \mathcal{A}(g)$ is continuous on $\mathcal{S}(\mathbb{R})$. \square

Definition 3.7 (Geometric Functional on $\mathcal{S}(\mathbb{R})$). For $g \in \mathcal{S}(\mathbb{R})$ even, the *geometric functional* is defined as

$$Q_{\text{geom}}(g) := P(g) - \mathcal{A}(g) + \tfrac{1}{2}g(0) + 2J(g) = P(g) + \int_0^\infty g_b(x) \rho_W(x) dx,$$

where ρ_W is as in (4.3) (see Proposition 4.6 for the constant audit).

3.2 Spectral and Zero Functionals

Theorem 3.8 (Maaß–Selberg PV pairing; atomlessness at $\tau = 0$). *In $\mathcal{S}'(\mathbb{R})$, taken in the symmetric principal-value sense,*

$$\varphi'(\tau) = \text{PV } 4 \text{ Re} \left(\frac{\Lambda'}{\Lambda}(2i\tau) \right), \quad \Lambda(s) = \pi^{-s/2} \Gamma\left(\frac{s}{2}\right) \zeta(s),$$

and there is no δ_0 atom at $\tau = 0$ in the Maaß–Selberg ledger. Consequently the spectral-shift measure

$$d\xi(\tau) := \frac{1}{2\pi} \varphi'(\tau) d\tau$$

is a tempered, atomless distribution, and pairings with even $g \in \mathcal{S}(\mathbb{R})$ are taken in the symmetric principal-value sense. Proof idea: boundary identification and local Poisson–kernel cancellation as in Thm. 2.4, together with Stirling bounds and the standard ζ'/ζ partial fractions.

Definition 3.9 (Spectral Functional). The *spectral functional* is

$$I(g) := \frac{1}{2\pi} \text{PV} \int_{\mathbb{R}} g(\tau) \varphi'(\tau) d\tau, \quad (\text{symmetric PV throughout})$$

$$\text{PV} \int_{\mathbb{R}} (\cdots) d\tau := \lim_{T \rightarrow \infty} \int_{-T}^T (\cdots) d\tau.$$

We use the symmetric PV. In the Maaß–Selberg ledger the spectral–shift measure is $d\xi(\tau) = \frac{1}{2\pi} \varphi'(\tau) d\tau$ and carries no δ_0 mass, so the PV acts only as a symmetric truncation. By Hypothesis (H.3), $\varphi'(\tau) = O(\log(2 + |\tau|))$, and $I(g)$ is welldefined and continuous on $\mathcal{S}(\mathbb{R})$.

See Thms. 2.4 and 3.8 for the boundary identity and the PV/no-atom lock.

Definition 3.10 (Weil Zero Functional). For a nontrivial zero $\rho = \beta + i\gamma$ of $\zeta(s)$, define the *one-sided zero weight*

$$\mathcal{H}(g; \rho) := \frac{1}{2\pi} \int_0^\infty e^{-\beta x/2} g_b(x) \cos(\gamma x/2) dx.$$

(Equivalently, via $y = x/2$: $\mathcal{H}(g; \rho) = \frac{1}{\pi} \int_0^\infty e^{-\beta y} g_b(2y) \cos(\gamma y) dy$.) The *Weil zero functional* is defined as the sum over zeros (counted with multiplicity):

$$\mathcal{W}(g) := 2 \sum_{\rho} \mathcal{H}(g; \rho).$$

Lemma 3.11 (Absolute convergence of the zero sum). *Let $g \in \mathcal{S}(\mathbb{R})$ be even. The sum defining $\mathcal{W}(g)$ converges absolutely: $\sum_{\rho} |\mathcal{H}(g; \rho)| < \infty$.*

Proof. Since $g_b \in \mathcal{S}(\mathbb{R})$, integration by parts shows that $\mathcal{H}(g; \beta + i\gamma) = O_m((1 + |\gamma|)^{-m})$ for any m , uniformly in $\beta \in [0, 1]$. Combining with the Riemann–von Mangoldt count yields $\sum_{\rho} |\mathcal{H}(g; \rho)| < \infty$ for $m \geq 3$. This implies that \mathcal{W} defines a tempered distribution and is thus a continuous functional on $\mathcal{S}(\mathbb{R})$. \square

Remark 3.12 (Continuity and Autocorrelations). If $g = g_{\Phi}$ with $\Phi \in \mathcal{S}(\mathbb{A})$, then by H.5, $g_{\Phi} \in \mathcal{S}(\mathbb{R}) \cap \mathcal{C}_W$, so the zero sum converges absolutely. The continuity of \mathcal{W} on $\mathcal{S}(\mathbb{R})$ is essential for the regularization argument in Section 6. If the approximants $g_{\Phi}^{(N,t)}$ converge to g_{Φ} in $\mathcal{S}(\mathbb{R})$ (Lemma 6.3), then $\mathcal{W}(g_{\Phi}^{(N,t)}) \rightarrow \mathcal{W}(g_{\Phi})$, ensuring the Explicit Formula extends to g_{Φ} in the Maaß–Selberg normalization.

3.3 The Explicit Formula and Identities

Theorem 3.13 (Asymmetric Explicit Formula (AEF) on \mathcal{A}_{BL}). *Let $g \in \mathcal{A}_{\text{BL}}$. In the Maaß–Selberg normalization, the following identity holds:*

$$\mathcal{W}(g) = Q_{\text{geom}}(g) \quad (\text{see Thm. 1.8 for the } Q_{\text{geom}} \text{ ledger}). \quad (3.4)$$

Proof. This is Hypothesis (H.1), established in Paper I under the adopted normalization. \square

Proposition 3.14 (Extension of AEF to Autocorrelations). *Let $\Phi \in \mathcal{S}(\mathbb{A})$. The autocorrelation $g_{\Phi} = \Phi * \tilde{\Phi}$ satisfies the asymmetric explicit formula:*

$$\mathcal{W}(g_{\Phi}) = Q_{\text{geom}}(g_{\Phi}). \quad (3.5)$$

Proof. By H. (H.5), $g_\Phi \in \mathcal{A}_{\text{Exp}} \subset \mathcal{S}(\mathbb{R})$. The Fejér–Gaussian regularization (Construction 6.1) provides a net $g_\Phi^{(N,t)} \in \mathcal{A}_{\text{BL}}$ converging to g_Φ . The convergence holds in $\mathcal{S}(\mathbb{R})$ (Lemma 6.3) and the transforms converge in $L^1(d\nu)$ (Lemma 6.4). The functional $\mathcal{W}(g)$ is continuous on $\mathcal{S}(\mathbb{R})$ (Lemma 6.8). The functional $Q_{\text{geom}}(g)$ is continuous in the $L^1(d\nu)$ topology (Lemma 6.8). By Theorem 3.13, the identity holds on the approximants: $\mathcal{W}(g_\Phi^{(N,t)}) = Q_{\text{geom}}(g_\Phi^{(N,t)})$. Taking the iterated limit and invoking continuity in the respective topologies (as detailed in Theorem 6.9) yields the result. \square

Lemma 3.15 (Spectral Handshake Identities on \mathcal{A}_{BL}). *For $g \in \mathcal{A}_{\text{BL}}$, the following identities hold:*

$$\begin{aligned} Q_{\text{geom}}(g) &= \mathcal{W}(g), \\ Q_{\text{geom}}(g) &= 2J(g) - I(g). \end{aligned}$$

Proof. The first identity is the AEF (Thm. 3.13). The second identity follows from the geometric relation $I(g) = \mathcal{A}(g) - \frac{1}{2}g(0) - P(g)$, established in the derivation of the AEF (Papers I-II), combined with the definition of $Q_{\text{geom}}(g)$. \square

4 The Mellin–Torsion Kernel and Geometric Density

Remark 4.1 (Domain and normalization of $C_{1/2}$). Throughout this section, $C_{1/2} = C_{1/2}$ denotes the Maaß–Selberg boundary operator at $s = \frac{1}{2}$, acting on even test profiles. We first define $C_{1/2}$ on $\mathcal{S}(\mathbb{R}) \cap \mathcal{C}_W$ (via the boundary kernel at infinity; cf. (H.(H.3))) and extend to \mathcal{C}_W by density using the Fejér–Gaussian scheme of Theorem 6.1. All pairings are taken in the *symmetric principal value* sense and with the Maaß–Selberg normalization used in (H.(H.3))–(H.(H.4)).

We now introduce the Mellin–torsion mechanism, which reveals the inherent positivity of the geometric functional by analyzing its structure on the modulus line $(0, \infty)$.

Definition 4.2 (Exponential semigroup operator). Let $x > 0$ denote the modulus variable. The exponential semigroup operator \mathbf{E}^a ($a \geq 0$) is defined by

$$(\mathbf{E}^a \phi)(x) := e^{-ax} \phi(x) \quad \text{for } \phi \in C_c^\infty(0, \infty);$$

by duality this extends to the space of distributions $\mathcal{D}'(0, \infty)$. The family $(\mathbf{E}^a)_{a \geq 0}$ consists of commuting multipliers.

The resolvent operator $(\text{Id} - \mathbf{E})^{-1}$ (where $\mathbf{E} := \mathbf{E}^1$) is given by the Neumann series $\sum_{n \geq 0} \mathbf{E}^n$, converging distributionally when acting on test functions $C_c^\infty(0, \infty)$.

Lemma 4.3 (Mellin–Torsion Operator Identity). *Define the Mellin–Torsion operator (Half-Shift operator) by*

$$C_{1/2} := (\text{Id} - \mathbf{E}^{1/2})(\text{Id} - \mathbf{E})^{-1}.$$

On $C_c^\infty(0, \infty)$ (functions supported away from $x = 0$), where $(\mathbf{E}^a \phi)(x) = e^{-ax} \phi(x)$, this operator acts as multiplication by the kernel $T_{1/2}(x)$:

$$T_{1/2}(x) = \frac{1}{1 + e^{-x/2}} = \frac{1 - e^{-x/2}}{1 - e^{-x}}, \quad x > 0. \quad (4.1)$$

This identity holds in the space of distributions $\mathcal{D}'(0, \infty)$. The Neumann series $\sum_{n \geq 0} \mathbf{E}^n$ converges when paired against $C_c^\infty(0, \infty)$ tests. Precisely, for $\psi, \phi \in C_c^\infty(0, \infty)$:

$$\langle (\text{Id} - \mathbf{E})^{-1} \psi, \phi \rangle := \sum_{n \geq 0} \langle \mathbf{E}^n \psi, \phi \rangle.$$

Since the support of ϕ is bounded away from zero (say $\text{supp}(\phi) \subset [a, b], a > 0$), we have $\|e^{-nx}\phi\|_{L^\infty} \leq e^{-na}\|\phi\|_{L^\infty}$. The convergence of the geometric series $\sum e^{-na}$ ensures absolute convergence of the pairing. By duality, $(\text{Id} - \mathbf{E})^{-1}$ defines a continuous operator on $\mathcal{D}'(0, \infty)$. With $(\text{Id} - \mathbf{E}) = (\text{Id} - \mathbf{E}^{1/2})(\text{Id} + \mathbf{E}^{1/2})$, we get $C_{1/2} = (\text{Id} + \mathbf{E}^{1/2})^{-1}$. The resulting multiplier $T_{1/2}(x)$ is smooth, bounded on $(0, \infty)$, and strictly positive.

Proof. Pointwise, the identity follows immediately from the algebraic factorization $(1 - e^{-x}) = (1 - e^{-x/2})(1 + e^{-x/2})$. Operatorially, we have $(\text{Id} - \mathbf{E}) = (\text{Id} - \mathbf{E}^{1/2})(\text{Id} + \mathbf{E}^{1/2})$. Since the operators commute,

$$C_{1/2} = (\text{Id} - \mathbf{E}^{1/2})[(\text{Id} - \mathbf{E}^{1/2})(\text{Id} + \mathbf{E}^{1/2})]^{-1} = (\text{Id} + \mathbf{E}^{1/2})^{-1}.$$

Multiplication by $(1 + e^{-x/2})^{-1}$ corresponds to the action of $(\text{Id} + \mathbf{E}^{1/2})^{-1}$. \square

Properties of the Torsion Kernel. The kernel $T_{1/2}(x)$ is strictly positive, smooth, and monotone on $(0, \infty)$ (see Figure 1 and Section A). This structure governs the continuous part of the geometric functional.

Definition 4.4 (Continuous geometric contribution). Define the continuous part of the geometric functional as

$$W_{\text{cont}}(g) := -\mathcal{A}(g) + \frac{1}{2}g(0) + 2J(g).$$

Proposition 4.5 (Archimedean functional via torsion). *The Archimedean functional $\mathcal{A}(g)$ admits the modulus-line representation*

$$\mathcal{A}(g) = \frac{1}{\pi} \int_0^\infty g_b(2x) \frac{e^{-x}}{1 + e^{-x}} dx. \quad (4.2)$$

Proof. Apply Hypothesis (H.2) with the modulus-line profile $W(u) = \frac{1}{\pi}(1 - e^{-u})g_b(2u)$ to obtain

$$\begin{aligned} \mathcal{A}(g) &= \int_0^\infty W(u) \frac{e^{-u}}{1 - e^{-2u}} du \\ &= \frac{1}{\pi} \int_0^\infty g_b(2u) \frac{e^{-u}(1 - e^{-u})}{(1 - e^{-u})(1 + e^{-u})} du \\ &= \frac{1}{\pi} \int_0^\infty g_b(2u) \frac{e^{-u}}{1 + e^{-u}} du. \end{aligned}$$

Relabel $u \mapsto x$ to match (4.2). \square

The following proposition is the central identity revealing the positivity structure.

Proposition 4.6 (Geometric density on the modulus line). *For an even $g \in \mathcal{S}(\mathbb{R})$, the continuous geometric contribution can be expressed as an integral against a strictly positive density $\rho_W(x)$:*

$$W_{\text{cont}}(g) = \int_0^\infty g_b(x) \rho_W(x) dx,$$

where

$$\rho_W(x) = \frac{1}{2\pi} \left(\frac{1}{1 + e^{-x/2}} + 2e^{-x/2} \right), \quad x > 0. \quad (4.3)$$

This is exactly the Maaß–Selberg continuous density recorded in Paper II (Eq. (4.3); see also Prop. 5.2 and the related remarks there). In particular, $\rho_W(x) > 0$ for all $x > 0$. Moreover, for every $\sigma > 0$,

$$\int_0^\infty \rho_W(x) e^{-\sigma x} dx = \frac{1}{2\pi} \left(\int_0^\infty \frac{e^{-\sigma x}}{1 + e^{-x/2}} dx + \frac{2}{\sigma + \frac{1}{2}} \right) < \infty,$$

a bound used in the dominated convergence steps below.

Proof. We utilize Hypothesis (H.2) (Archimedean dictionary). The Archimedean functional $\mathcal{A}(g)$ corresponds to the pairing

$$\mathcal{A}(g) = \int_0^\infty W(u) \frac{e^{-u}}{1 - e^{-2u}} du,$$

where the modulus-line profile is $W(u) = \frac{1}{\pi}(1 - e^{-u})g_b(2u)$ for $u > 0$. *The integral converges absolutely.* Near $u = 0$, the kernel behaves as $\frac{e^{-u}}{1 - e^{-2u}} = \frac{1}{2u} + O(1)$. Since $g \in \mathcal{S}(\mathbb{R})$, g_b is continuous, and $W(u) = \frac{1}{\pi}(u + O(u^2))g_b(0) = O(u)$. Thus the integrand is $O(1)$ near $u = 0$. The apparent singularity is removable, and the integral does not require a PV interpretation on the modulus line. Substituting $W(u)$ yields

$$\begin{aligned} \mathcal{A}(g) &= \frac{1}{\pi} \int_0^\infty (1 - e^{-u})g_b(2u) \frac{e^{-u}}{(1 - e^{-u})(1 + e^{-u})} du \\ &= \frac{1}{\pi} \int_0^\infty \frac{e^{-u}}{1 + e^{-u}} g_b(2u) du. \end{aligned}$$

Using the algebraic identity $\frac{e^{-u}}{1 + e^{-u}} = 1 - \frac{1}{1 + e^{-u}}$ and recognizing that $\frac{1}{\pi} \int_0^\infty g_b(2u) du = \frac{1}{2}g(0)$ (by Thm. 2.8), we obtain

$$\mathcal{A}(g) = \frac{1}{2}g(0) - \frac{1}{\pi} \int_0^\infty \frac{1}{1 + e^{-u}} g_b(2u) du.$$

Therefore, the first two terms of $W_{\text{cont}}(g)$ isolate the torsion kernel:

$$-\mathcal{A}(g) + \frac{1}{2}g(0) = \frac{1}{\pi} \int_0^\infty \frac{1}{1 + e^{-u}} g_b(2u) du.$$

From (3.3), the boundary term is $2J(g) = \frac{2}{\pi} \int_0^\infty e^{-u} g_b(2u) du$. Combining these gives

$$W_{\text{cont}}(g) = \frac{1}{\pi} \int_0^\infty \left(\frac{1}{1 + e^{-u}} + 2e^{-u} \right) g_b(2u) du.$$

Changing variables $x = 2u$ yields the desired expression:

$$W_{\text{cont}}(g) = \frac{1}{2\pi} \int_0^\infty \left(\frac{1}{1 + e^{-x/2}} + 2e^{-x/2} \right) g_b(x) dx,$$

which matches the Maaß–Selberg density recorded in the companion paper (Eq. (5.6)). Since $e^{-x/2} > 0$ for $x > 0$, the density $\rho_W(x)$ is strictly positive. \square

Remark 4.7 (Numerical verification). Section D details a computational verification of this identity using randomized band-limited tests, confirming the result to machine precision. Equivalently, in the mixed measure topology one may view the entire geometric functional as the $L^1(d\nu)$ pairing $Q_{\text{geom}}(g) = \int g_b d\nu$; see Definitions 3.7, 4.8 and Lemma 4.9.

Definition 4.8 (Prime-continuous Weil measure). Define the positive Borel measure on $(0, \infty)$ by

$$d\nu(x) := \rho_W(x) dx + \frac{1}{\pi} \sum_p \sum_{k \geq 1} (\log p)(1 - p^{-k}) \delta_{2k \log p},$$

with atoms at the lattice sites $x = 2k \log p$, where ρ_W is the density in (4.3). For $g_b \in C((0, \infty)) \cap L^1(\rho_W dx)$ we evaluate $\int g_b d\nu$ by pointwise values at the atomic lattice $\{2k \log p\}$, which are canonical since g_b is continuous; for general $L^1(d\nu)$ data we use disjoint C_c^∞ bump approximations

to realize atomic evaluations (cf. Lem. 4.9). Then the geometric functional can be written as the $L^1(d\nu)$ pairing

$$Q_{\text{geom}}(g) = \int_{(0,\infty)} g_{\text{b}}(x) d\nu(x)$$

whenever the right-hand side is absolutely convergent.

Lemma 4.9 ($L^1(d\nu)$ continuity and density). *Let $d\nu = \rho_W(x) dx + \frac{1}{\pi} \sum_p \sum_{k \geq 1} (\log p)(1-p^{-k}) \delta_{2k \log p}$. (i) If $g_{\text{b}} \in L^1(d\nu)$, then $|\int g_{\text{b}} d\nu| \leq \|g_{\text{b}}\|_{L^1(d\nu)}$, so the map $g_{\text{b}} \mapsto \int g_{\text{b}} d\nu$ is continuous. (ii) $C_c^\infty((0,\infty))$ is dense in $L^1(d\nu)$; in particular, $L^1(d\nu)$ convergence forces weighted ℓ^1 convergence of atomic values.*

Proof. (i) Immediate from the definition of the $L^1(d\nu)$ norm. (ii) Write $\|\cdot\|_{L^1(d\nu)} = \|\cdot\|_{L^1(\rho_W dx)} + \|\cdot\|_{\ell^1(\text{atoms})}$. For the continuous part, $C_c^\infty((0,\infty))$ is dense in $L^1(\rho_W dx)$.

Bounded weight. By Appendix A, Lemma A.1,

$$\frac{1}{2\pi} < \rho_W(x) < \frac{5}{4\pi} \quad (x > 0).$$

Thus, the $L^1(\rho_W dx)$ norm is equivalent to the unweighted $L^1(dx)$ norm on $(0,\infty)$. *Atomic approximation.* For the atomic part, fix $\varepsilon > 0$. Let $h_c \in C_c^\infty((0,\infty))$ approximate g_{b} such that $\|g_{\text{b}} - h_c\|_{L^1(\rho_W dx)} < \varepsilon/3$. Choose a finite lattice set $L_M = \{2k \log p\}$ such that the weighted ℓ^1 norm of g_{b} on the tail (outside L_M) is $< \varepsilon/3$. Let $C_M = \sum_{x_j \in L_M} |g_{\text{b}}(x_j) - h_c(x_j)|$. If $C_M > 0$, let $C_\rho = \|\rho_W\|_\infty$ (finite by Lemma A.1). Choose $\delta > 0$ small enough such that the intervals $(x_j - \delta, x_j + \delta)$ are disjoint and contained in $(0,\infty)$, and such that $2\delta C_\rho < \frac{\varepsilon}{3C_M}$. For each $x_j \in L_M$, pick a smooth bump $\eta_j \in C_c^\infty((x_j - \delta, x_j + \delta))$ with $\eta_j(x_j) = 1$ and $0 \leq \eta_j \leq 1$. Then

$$\int \eta_j(x) \rho_W(x) dx \leq 2\delta C_\rho < \frac{\varepsilon}{3C_M}.$$

Define the adjustment $h_a(x) := \sum_{x_j \in L_M} (g_{\text{b}}(x_j) - h_c(x_j)) \eta_j(x)$. Then $h := h_c + h_a \in C_c^\infty((0,\infty))$. This ensures $h(x_j) = g_{\text{b}}(x_j)$ on L_M . The continuous error introduced by h_a is bounded by $\|h_a\|_{L^1(\rho_W dx)} < C_M \cdot \frac{\varepsilon}{3C_M} = \varepsilon/3$. The total error $\|g_{\text{b}} - h\|_{L^1(d\nu)}$ is the sum of the continuous error ($\|g_{\text{b}} - h\|_{L^1(\rho_W dx)} \leq \|g_{\text{b}} - h_c\| + \|h_a\| < 2\varepsilon/3$) and the atomic error (zero on L_M , $< \varepsilon/3$ on the tail), totaling $< \varepsilon$. \square

5 Positivity on the Band-Limited Weil Cone

The decomposition derived in Section 4 immediately yields positivity on the restricted class \mathcal{A}_{BL} . This proves Thm. 1.2 and Thm. 1.3.

Theorem 5.1 (Band-limited positivity). *If $g \in \mathcal{C}_W \cap \mathcal{A}_{\text{BL}}$, then $Q_{\text{geom}}(g) \geq 0$.*

Proof. Let $g \in \mathcal{C}_W \cap \mathcal{A}_{\text{BL}}$. By Thm. 2.8, $g_{\text{b}}(x) \geq 0$ for all $x \in \mathbb{R}$. The geometric functional is $Q_{\text{geom}}(g) = P(g) + W_{\text{cont}}(g)$.

Positivity of the Prime Block $P(g)$. From Eq. (3.1), $P(g)$ is a sum of terms involving $g_{\text{b}}(x)$ evaluated at $x = 2k \log p$. The coefficients $(\log p)(1-p^{-k})/\pi$ are strictly positive. Since $g_{\text{b}} \geq 0$, $P(g) \geq 0$. (As $g \in \mathcal{A}_{\text{BL}}$, this is a finite sum.)

Positivity of the Continuous Block $W_{\text{cont}}(g)$. By Thm. 4.6,

$$W_{\text{cont}}(g) = \int_0^\infty g_{\text{b}}(x) \rho_W(x) dx.$$

Since $g_{\text{b}}(x) \geq 0$ and $\rho_W(x) > 0$ for $x > 0$, the integrand is non-negative, and thus $W_{\text{cont}}(g) \geq 0$.

Therefore, $Q_{\text{geom}}(g) \geq 0$. \square

Corollary 5.2 (Weil Positivity on \mathcal{A}_{BL}). *If $g \in \mathcal{C}_W \cap \mathcal{A}_{\text{BL}}$, then $\mathcal{W}(g) \geq 0$.*

Proof. By the Spectral Handshake on \mathcal{A}_{BL} (Thm. 3.15), $\mathcal{W}(g) = Q_{\text{geom}}(g)$. The result follows from Thm. 5.1. \square

6 Regularization, Positivity on \mathcal{C}_W , and the Spectral Handshake

To extend the positivity result from the dense subspace \mathcal{A}_{BL} to the full Weil cone \mathcal{C}_W , we employ a rigorous regularization procedure. This Fejér–Gaussian scheme constructs an approximation of the identity that preserves positive definiteness while enforcing smoothness and compact support on the transform side (the measure side), ensuring the approximations land in $\mathcal{C}_W \cap \mathcal{A}_{\text{BL}}$.

Overview of the Strategy. The strategy relies on continuity in appropriate topologies for both sides of the Explicit Formula. To extend the AEF identity $\mathcal{W}(g) = Q_{\text{geom}}(g)$ from \mathcal{A}_{BL} to autocorrelations g_Φ , we utilize the convergence of the regularization in the Schwartz topology $\mathcal{S}(\mathbb{R})$ (required for the continuity of \mathcal{W}) and in the $L^1(d\nu)$ topology (required for the continuity of Q_{geom}).

1. Define a smooth regularization $g^{(N,t)} \in \mathcal{C}_W \cap \mathcal{A}_{\text{BL}}$ (Thm. 6.1).
2. Establish $g^{(N,t)} \rightarrow g_\Phi$ in $\mathcal{S}(\mathbb{R})$ (Lemma 6.3).
3. Confirm continuity of Q_{geom} and \mathcal{W} on $\mathcal{S}(\mathbb{R})$ (Lemma 6.8).
4. Pass the AEF identity from $g^{(N,t)}$ to g_Φ by continuity (Theorem 6.9).
5. Since $g^{(N,t)} \in \mathcal{C}_W \cap \mathcal{A}_{\text{BL}}$, we have $Q_{\text{geom}}(g^{(N,t)}) \geq 0$ (by Theorem 5.1). Continuity yields $Q_{\text{geom}}(g_\Phi) \geq 0$ (Theorem 6.11).

6.1 The Fejér–Gaussian Regularization Scheme

Continuity reminder. Whenever $g^{(N,t)} \rightarrow g$ in the mixed weak-* / $L^1(d\nu)$ topology (as in Theorem 6.1), each component of $Q_{\text{geom}}(g)$ is continuous along the net, so $Q_{\text{geom}}(g^{(N,t)}) \rightarrow Q_{\text{geom}}(g)$.

Construction 6.1 (Smooth regularization scheme). Let $g \in \mathcal{C}_W \cap \mathcal{S}(\mathbb{R})$ (e.g., an autocorrelation g_Φ) with Bochner measure μ_g . We define a regularization indexed by $t > 0$ (smoothing scale) and $N \in \mathbb{N}$ (cutoff scale index, with $R_N \uparrow \infty$ and $R_1 \geq 1$).

1. **Mollification (Gaussian aspect).** Define the standard Gaussian kernel $G_t(x) = \frac{1}{\sqrt{4\pi t}} e^{-x^2/(4t)}$, an approximate identity as $t \downarrow 0$. Set the smoothed density

$$u_t(x) := (G_t * \mu_g)(x).$$

(If $g \in \mathcal{S}(\mathbb{R})$, such as an autocorrelation g_Φ , then $d\mu_g(x) = \frac{1}{2\pi} g_b(|x|) dx$ by Lemma 2.8, and $u_t(x) = \frac{1}{2\pi} (G_t * g_b)(x)$.) Then $u_t \in C^\infty(\mathbb{R})$ is even, nonnegative, and integrable ($\|u_t\|_{L^1} = \|\mu_g\| < \infty$). Crucially, its derivatives are also integrable: $\|\partial_x^j u_t\|_{L^1} < \infty$. As $t \downarrow 0$, the measure $u_t dx \rightarrow \mu_g$ weakly-*

2. **Smooth Cutoff (Fejér aspect).** Let $\phi \in C_c^\infty(\mathbb{R})$ be an even plateau function: $0 \leq \phi \leq 1$, $\phi \equiv 1$ on $[-1, 1]$, $\text{supp } \phi \subset [-2, 2]$, and assume $\phi(x)$ is non-increasing for $x \geq 0$. Define the scaled cutoff

$$\eta_N(x) := \phi(x/R_N).$$

Then $\eta_N(x)$ is non-decreasing in N for fixed x (i.e., $0 \leq \eta_N(x) \leq \eta_{N+1}(x) \leq 1$), and $\eta_N \rightarrow 1$ pointwise as $N \rightarrow \infty$. The derivatives satisfy the bounds $\|\partial_x^k \eta_N\|_\infty \ll_k R_N^{-k}$ for $k \geq 1$.

Define the regularized measure and the corresponding test function:

$$d\mu^{(N,t)}(x) := \eta_N(x) u_t(x) dx, \quad g^{(N,t)} := \widehat{\mu^{(N,t)}}.$$

Lemma 6.2 (Properties of the regularization). *The regularized function $g^{(N,t)}$ satisfies the following properties:*

1. $g^{(N,t)}$ is even and $g^{(N,t)} \in \mathcal{C}_W \cap \mathcal{A}_{BL}$.
2. The cosine transform is $g_b^{(N,t)}(x) = 2\pi \eta_N(|x|) u_t(|x|)$. It is even, nonnegative, and belongs to $C_c^\infty(\mathbb{R})$.
3. $g^{(N,t)} \rightarrow g$ in the weak-* topology of $\mathcal{S}'(\mathbb{R})$ as $N \rightarrow \infty$ and $t \downarrow 0$; equivalently, $\mu^{(N,t)} \rightarrow \mu_g$ as finite Borel measures and $\widehat{g^{(N,t)}} = 2\pi \eta_N(|\cdot|) u_t(|\cdot|) \rightarrow 2\pi \frac{d\mu_g}{dx}$ in the sense of distributions (pointwise a.e. where μ_g has a density). If in addition $g \in \mathcal{S}(\mathbb{R})$, then the convergence holds in the Schwartz topology $\mathcal{S}(\mathbb{R})$ under the iterated limit (Lemma 6.3).

Proof. 1-2. The measure $\mu^{(N,t)}$ is absolutely continuous, even, finite, nonnegative, and compactly supported. Its density is smooth and compactly supported, hence $g_b^{(N,t)} \in C_c^\infty(\mathbb{R})$. This confirms $g^{(N,t)} \in \mathcal{C}_W \cap \mathcal{A}_{BL}$. 3. The convergence follows from the construction: $\mu^{(N,t)} \rightarrow u_t dx$ as $N \rightarrow \infty$ (by MCT), and $u_t dx \rightarrow \mu_g$ as $t \downarrow 0$ (weak-* convergence). \square

Lemma 6.3 (Schwartz convergence for autocorrelations). *Let g_Φ be an autocorrelation. By H.5, $g_\Phi \in \mathcal{S}(\mathbb{R}) \cap \mathcal{C}_W$. The Fejér–Gaussian approximants $g_\Phi^{(N,t)}$ converge to g_Φ in the topology of $\mathcal{S}(\mathbb{R})$ under the iterated limit $N \rightarrow \infty$, then $t \downarrow 0$.*

Proof. We work on the transform side. The availability of the strong Schwartz topology (H.5) is crucial here, as it ensures the continuity of the functionals \mathcal{W} and Q_{geom} . Since $g_\Phi \in \mathcal{S}(\mathbb{R})$, its Bochner measure is $d\mu_{g_\Phi} = \frac{1}{2\pi}(g_\Phi)_b dx$ (Lemma 2.8). The regularization (Construction 6.1) defines $u_t = G_t * \mu_{g_\Phi} = \frac{1}{2\pi}(G_t * (g_\Phi)_b)$. Let $v_t := G_t * (g_\Phi)_b = 2\pi u_t$. By Lemma 6.2, the transform of the approximation is $(g_\Phi^{(N,t)})_b = 2\pi \eta_N u_t = \eta_N v_t$.

We show $(g_\Phi^{(N,t)})_b \rightarrow (g_\Phi)_b$ in $\mathcal{S}(\mathbb{R})$. Since $(g_\Phi)_b \in \mathcal{S}(\mathbb{R})$, $v_t \rightarrow (g_\Phi)_b$ in $\mathcal{S}(\mathbb{R})$ as $t \downarrow 0$ (Gaussian approximate-identity property on the Schwartz space). For fixed $t > 0$, $v_t \in \mathcal{S}(\mathbb{R})$. We show $\eta_N v_t \rightarrow v_t$ in $\mathcal{S}(\mathbb{R})$ as $N \rightarrow \infty$. For any Schwartz seminorm $p_{\alpha,\beta}(h) = \sup_{x \in \mathbb{R}} |x^\alpha \partial^\beta h(x)|$, consider $h_N = (1 - \eta_N)v_t$. By the Leibniz rule,

$$\partial^\beta h_N(x) = \sum_{k=0}^{\beta} \binom{\beta}{k} \partial^k (1 - \eta_N)(x) \partial^{\beta-k} v_t(x).$$

We analyze the convergence $p_{\alpha,\beta}(h_N) \rightarrow 0$.

Case $k = 0$: The term is $(1 - \eta_N) \partial^\beta v_t$. Since $1 - \eta_N$ is supported on $|x| \geq R_N$,

$$\sup_{x \in \mathbb{R}} |x^\alpha (1 - \eta_N(x)) \partial^\beta v_t(x)| \leq \sup_{|x| \geq R_N} |x^\alpha \partial^\beta v_t(x)|.$$

This vanishes as $N \rightarrow \infty$ because $v_t \in \mathcal{S}(\mathbb{R})$.

Case $k \geq 1$: $\partial^k (1 - \eta_N)$ is supported on the transition region (e.g., $R_N \leq |x| \leq 2R_N$), with bounds $\|\partial^k (1 - \eta_N)\|_\infty \ll_k R_N^{-k}$. Hence

$$\sup_{x \in \mathbb{R}} |x^\alpha \partial^k (1 - \eta_N)(x) \partial^{\beta-k} v_t(x)| \ll_{\alpha,\beta,k} R_N^{\alpha-k} \sup_{|x| \geq R_N} |\partial^{\beta-k} v_t(x)|.$$

This converges to 0 as $N \rightarrow \infty$, since the rapid decay of v_t overcomes the polynomial growth $R_N^{\alpha-k}$.

Therefore $p_{\alpha,\beta}(h_N) \rightarrow 0$ and $\eta_N v_t \rightarrow v_t$ in $\mathcal{S}(\mathbb{R})$. Iterating the limits gives the convergence of the transforms in $\mathcal{S}(\mathbb{R})$. Since the Fourier transform is a topological isomorphism on $\mathcal{S}(\mathbb{R})$, $g_\Phi^{(N,t)} \rightarrow g_\Phi$ in $\mathcal{S}(\mathbb{R})$. \square

Lemma 6.4 ($L^1(d\nu)$ convergence for autocorrelations). *Let g_Φ be an autocorrelation. By H.5, $g_\Phi \in \mathcal{A}_{\text{Exp}}$. The transforms of the Fejér–Gaussian approximants $(g_\Phi^{(N,t)})_{\text{b}}$ converge to $(g_\Phi)_{\text{b}}$ in the topology of $L^1(d\nu)$ under the iterated limit $N \rightarrow \infty$, then $t \downarrow 0$.*

Proof. Let $g_{\text{b}} = (g_\Phi)_{\text{b}}$ and $g_{\text{b}}^{(N,t)} = (g_\Phi^{(N,t)})_{\text{b}}$. We have $g_{\text{b}}^{(N,t)} = \eta_N v_t$, where $v_t = G_t * g_{\text{b}}$ (using the Gaussian kernel G_t). Since $g_\Phi \in \mathcal{A}_{\text{Exp}}$ (H.5), $|g_{\text{b}}(x)| \leq C e^{-\sigma|x|}$ with $\sigma > 1/2$.

Step 0: Uniform Domination. We must show v_t is uniformly dominated by a function in $L^1(d\nu)$ for $t \in (0, 1]$. Using the inequality $e^{-\sigma|y|} \leq e^{-\sigma|x|} e^{\sigma|x-y|}$, we have

$$|v_t(x)| \leq C \int G_t(x-y) e^{-\sigma|y|} dy \leq C e^{-\sigma|x|} \int G_t(z) e^{\sigma|z|} dz.$$

The integral $I_t = \int_{\mathbb{R}} G_t(z) e^{\sigma|z|} dz$ is finite. By completing the square in the exponent ($-\frac{z^2}{4t} + \sigma z = -\frac{(z-2t\sigma)^2}{4t} + \sigma^2 t$ for $z > 0$), we find

$$I_t = 2 \int_0^\infty \frac{1}{\sqrt{4\pi t}} e^{-z^2/(4t) + \sigma z} dz = 2e^{\sigma^2 t} \int_0^\infty \frac{1}{\sqrt{4\pi t}} e^{-(z-2t\sigma)^2/(4t)} dz \leq 2e^{\sigma^2 t}.$$

Thus $|v_t(x)| \leq 2C e^{\sigma^2 t} e^{-\sigma|x|}$. For $t \in (0, 1]$, $C' = 2C e^{\sigma^2}$ provides a uniform bound. The dominating function $M(x) = C' e^{-\sigma|x|}$ must be in $L^1(d\nu)$. Crucially, this relies on the strict condition $\sigma > 1/2$ (from H.5). This condition is necessary for integrability against the atomic prime measure component of $d\nu$; specifically, the weighted ℓ^1 sum over the primes converges absolutely only if $2\sigma > 1$ (cf. Lemma 3.2). This confirms $v_t \in L^1(d\nu)$ uniformly in t .

Step 1: $N \rightarrow \infty$ (fixed t). Since $v_t \in L^1(d\nu)$, and $0 \leq \eta_N \leq 1$ with $\eta_N \rightarrow 1$ pointwise, the Dominated Convergence Theorem (for $d\nu$) implies $\|g_{\text{b}}^{(N,t)} - v_t\|_{L^1(d\nu)} \rightarrow 0$.

Step 2: $t \downarrow 0$. We show $v_t \rightarrow g_{\text{b}}$ in $L^1(d\nu)$. G_t is an approximate identity, so $v_t \rightarrow g_{\text{b}}$ in $L^1(\mathbb{R})$, hence in $L^1(\rho_W dx)$. For the atomic part, $v_t(x) \rightarrow g_{\text{b}}(x)$ pointwise. By Step 0, $|v_t(x)|$ is uniformly dominated by $M(x) \in L^1(d\nu)$. By dominated convergence for the weighted ℓ^1 sum, the convergence holds in $L^1(d\nu)$.

Iterating the limits confirms the convergence. \square

To ensure the AEF applies to $g^{(N,t)}$, we verify that $g^{(N,t)}$ retains rapid decay, ensuring convergence of the spectral integral $I(g^{(N,t)})$.

Lemma 6.5 (Uniform Fourier decay at fixed t). *Fix $t > 0$. For every integer $m \geq 1$, there exists a constant $C_m(t) > 0$, independent of N (and of the plateau family (η_N) for fixed t), such that*

$$|g^{(N,t)}(\tau)| \leq C_m(t) (1 + |\tau|)^{-m} \quad (\tau \in \mathbb{R}).$$

Proof. We analyze $g^{(N,t)}(\tau) = \widehat{\mu^{(N,t)}}(\tau)$. Integrating by parts m times (valid since the density is C_c^∞) yields

$$(i\tau)^m g^{(N,t)}(\tau) = \int_{\mathbb{R}} e^{ix\tau} \partial_x^m (\eta_N u_t)(x) dx.$$

We must show that $\|\partial_x^m(\eta_N u_t)\|_{L^1}$ is bounded uniformly in N for fixed t . By the Leibniz rule,

$$\partial_x^m(\eta_N u_t) = \sum_{k=0}^m \binom{m}{k} (\partial_x^k \eta_N) (\partial_x^{m-k} u_t).$$

Taking L^1 norms gives the explicit bound

$$\|\partial_x^m(\eta_N u_t)\|_{L^1} \leq \sum_{k=0}^m \binom{m}{k} \|\partial_x^k \eta_N\|_{\infty} \|\partial_x^{m-k} u_t\|_{L^1}.$$

We examine the L^1 norm of each term. For fixed $t > 0$, $u_t \in C^\infty$ with $\|\partial_x^j u_t\|_{L^1} < \infty$ for all j .

Term $k = 0$: $\|\eta_N \partial_x^m u_t\|_{L^1} \leq \|\partial_x^m u_t\|_{L^1}$.

Terms $k \geq 1$: Using $\|\partial_x^k \eta_N\|_{\infty} \ll_k R_N^{-k}$ and $R_N \geq R_1 > 0$,

$$\|(\partial_x^k \eta_N) (\partial_x^{m-k} u_t)\|_{L^1} \ll_k \|\partial_x^{m-k} u_t\|_{L^1}.$$

Summing over k shows $\sup_N \|\partial_x^m(\eta_N u_t)\|_{L^1} < \infty$. Hence $|g^{(N,t)}(\tau)| \ll_m (1 + |\tau|)^{-m}$ uniformly in N . \square

Remark 6.6 (Role of Uniform Decay). Theorem 6.5 confirms that $g^{(N,t)} \in \mathcal{S}(\mathbb{R})$. This ensures the absolute convergence of the spectral integral $I(g^{(N,t)})$ (given H.(H.3)) and the zero sum $\mathcal{W}(g^{(N,t)})$, validating the application of the AEF identities (Thm. 3.15) to the approximations $g^{(N,t)}$.

6.2 Continuity and the Spectral Handshake on Autocorrelations

We define Q_{geom} on \mathcal{C}_W through the positive measure $d\nu$ and make the limit mechanism explicit in the only two places it matters: monotone convergence in N (cutoff scale) and approximate-identity continuity in t (mollification). Constants/normalizations are unchanged.

Definition 6.7 (Geometric functional on \mathcal{C}_W via positive measure). Let D_{geom} be the positive distribution defined by the measure $d\nu$ (Def. 4.8), acting by $\langle D_{\text{geom}}, \phi \rangle = \int_{(0,\infty)} \phi(x) d\nu(x)$. For $g \in \mathcal{S}(\mathbb{R}) \cap \mathcal{C}_W$ (including autocorrelations g_{b}), $Q_{\text{geom}}(g) = \langle D_{\text{geom}}, g_{\text{b}} \rangle$. The Fejér–Gaussian regularization $(g^{(N,t)})$ from Thm. 6.1 confirms the continuity of this functional under the approximation scheme:

$$Q_{\text{geom}}(g) = \lim_{t \downarrow 0} \lim_{N \rightarrow \infty} Q_{\text{geom}}(g^{(N,t)}).$$

By Lemma 6.10 (and the convergence in $\mathcal{S}(\mathbb{R})$ from Lemma 6.3), this iterated limit exists and confirms the value defined by the direct pairing.

Lemma 6.8 (Continuity of Functionals). *The functionals $W_{\text{cont}}(g)$ and $\mathcal{W}(g)$ define tempered distributions and are continuous on $\mathcal{S}(\mathbb{R})$. The functionals $P(g)$ and $Q_{\text{geom}}(g)$ are well-defined on \mathcal{A}_{Exp} and continuous with respect to the $L^1(d\nu)$ topology on the transforms g_{b} .*

Proof. $W_{\text{cont}}(g)$: The density $\rho_W(x)$ is bounded (Lemma A.1), hence defines a tempered distribution. The pairing $\langle \rho_W, g_{\text{b}} \rangle$ is continuous on $\mathcal{S}(\mathbb{R})$ (acting on g_{b}). Thus $g \mapsto W_{\text{cont}}(g)$ is continuous on $\mathcal{S}(\mathbb{R})$.

$\mathcal{W}(g)$: Absolute convergence on $\mathcal{S}(\mathbb{R})$ (Lemma 3.11) implies \mathcal{W} is a tempered distribution, hence continuous on $\mathcal{S}(\mathbb{R})$.

$P(g)$ and $Q_{\text{geom}}(g)$: These are defined on \mathcal{A}_{Exp} (Lemma 3.2). $Q_{\text{geom}}(g) = \int g_{\text{b}}(x) d\nu(x)$. By Lemma 4.9, this pairing is continuous with respect to the $L^1(d\nu)$ norm of g_{b} . \square

Theorem 6.9 (Spectral Handshake Extension to Autocorrelations). *Let $\Phi \in \mathcal{S}(\mathbb{A})$ and g_Φ be the autocorrelation. The identity $\mathcal{W}(g_\Phi) = Q_{\text{geom}}(g_\Phi)$ holds.*

Proof. Let $g^{(N,t)}$ be the Fejér–Gaussian approximants for g_Φ (Construction 6.1). By Lemma 6.2, $g^{(N,t)} \in \mathcal{A}_{\text{BL}}$. By the AEF on \mathcal{A}_{BL} (Theorem 3.13), we have

$$\mathcal{W}(g^{(N,t)}) = Q_{\text{geom}}(g^{(N,t)}).$$

We analyze the convergence of both sides under the iterated limit ($N \rightarrow \infty$, then $t \downarrow 0$).

Convergence of \mathcal{W} : By Lemma 6.3, $g^{(N,t)} \rightarrow g_\Phi$ in $\mathcal{S}(\mathbb{R})$. By Lemma 6.8, \mathcal{W} is continuous on $\mathcal{S}(\mathbb{R})$. Thus $\lim \mathcal{W}(g^{(N,t)}) = \mathcal{W}(g_\Phi)$.

Convergence of Q_{geom} : By Lemma 6.4, $(g^{(N,t)})_{\text{b}} \rightarrow (g_\Phi)_{\text{b}}$ in $L^1(d\nu)$. By Lemma 6.8, Q_{geom} is continuous in the $L^1(d\nu)$ topology. Thus $\lim Q_{\text{geom}}(g^{(N,t)}) = Q_{\text{geom}}(g_\Phi)$.

Taking the iterated limit of the identity above yields $\mathcal{W}(g_\Phi) = Q_{\text{geom}}(g_\Phi)$. \square

Lemma 6.10 (Existence and schemeindependence). *Fix $t > 0$. Then $N \mapsto \langle D_{\text{geom}}, (g^{(N,t)})_{\text{b}} \rangle$ increases to $\langle D_{\text{geom}}, (g^{(\infty,t)})_{\text{b}} \rangle$ with $\eta_N \rightarrow 1$. As $t \downarrow 0$,*

$$\int_0^\infty \rho_W(x) u_t(x) dx = \int_0^\infty (\rho_W * \tilde{\kappa}_t)(x) d\mu_g(x) \longrightarrow \int_0^\infty \rho_W(x) d\mu_g(x),$$

by the approximate-identity property of the mollifiers κ_t acting on finite measures. For any fixed $\sigma > 1/2$, the prime block is uniformly absolutely convergent by $\sum_{n \geq 2} \Lambda(n) n^{-2\sigma} < \infty$. Hence the iterated limit exists and is schemeindependent.

Theorem 6.11 (Positivity on the autocorrelation subcone). *For $\Phi \in \mathcal{S}(\mathbb{A})$, let $g_\Phi = \Phi * \tilde{\Phi}$. Then $Q_{\text{geom}}(g_\Phi) \geq 0$.*

Proof. By construction (H.5 and Definition 2.7), $g_\Phi \in \mathcal{A}_{\text{Exp}} \cap \mathcal{C}_W$. Let $g^{(N,t)}$ be the approximants for g_Φ . By Lemma 6.2, $g^{(N,t)} \in \mathcal{C}_W \cap \mathcal{A}_{\text{BL}}$. By Theorem 5.1 (Positivity on \mathcal{A}_{BL}), $Q_{\text{geom}}(g^{(N,t)}) \geq 0$ for all N, t . Since Q_{geom} is continuous in the $L^1(d\nu)$ topology (Lemma 6.8) and $(g^{(N,t)})_{\text{b}} \rightarrow (g_\Phi)_{\text{b}}$ in $L^1(d\nu)$ (Lemma 6.4), taking the limit preserves the inequality:

$$Q_{\text{geom}}(g_\Phi) = \lim_{t \downarrow 0} \lim_{N \rightarrow \infty} Q_{\text{geom}}(g^{(N,t)}) \geq 0.$$

\square

Finiteness. Since $g_\Phi \in \mathcal{A}_{\text{Exp}}$, the functionals $Q_{\text{geom}}(g_\Phi)$ and $\mathcal{W}(g_\Phi)$ are finite (Lemma 6.8).

Theorem 6.12 (Spectral handshake on \mathcal{A}_{BL} ; autocorrelation bridge). *For $g \in \mathcal{A}_{\text{BL}}$, $Q_{\text{geom}}(g) = \mathcal{W}(g) = 2J(g) - I(g)$ (PV). For g_Φ with $\Phi \in \mathcal{S}(\mathbb{A})$,*

$$\mathcal{Q}(\Phi) = P(g_\Phi) - \mathcal{A}(g_\Phi), \quad \mathcal{W}(g_\Phi) = Q_{\text{geom}}(g_\Phi).$$

Proof. \mathcal{A}_{BL} case: Thm. 3.13. Autocorrelations: (i) $g_\Phi \in \mathcal{A}_{\text{Exp}} \cap \mathcal{C}_W$ and $\sum_\rho |H(g_\Phi; \rho)| < \infty$ (Thm. 3.11); (ii) placebyplace ledger identifies P and \mathcal{A} with constants so that $-\mathcal{A} + \frac{1}{2}g(0) + 2J = \int g_{\text{b}} \rho_W$ with ρ_W exactly as in Paper II Eq. (5.6)/(2.9); (iii) the symmetric EF holds in the Maaß–Selberg normalization. (Companion crosscheck: Paper II, §§4–5 and App. A [6]). \square

7 Logical Closure: From Hypotheses to the Riemann Hypothesis

One-line bridge. $\forall \Phi : Q_{\text{geom}}(g_\Phi) \geq 0$ (Thm. 6.11) + EF identity $\mathcal{W}(g_\Phi) = Q_{\text{geom}}(g_\Phi)$ (Thm. 6.12) $\Rightarrow \mathcal{W}(g_\Phi) \geq 0$ for all Φ , and by (H.(H.4)) the Riemann Hypothesis holds.

We explicitly detail the logical flow from the standing hypotheses ((H.1))–((H.3)) to the Clay Millennium Riemann Hypothesis (via (H.4)).

Autocorrelation Positivity (Thm. 6.11) + *Bridge* (Thm. 7.1) $\Rightarrow \mathcal{W}(g_\Phi) \geq 0 \iff RH$ (H.(H.4)).

Lemma 7.1 (Coverage of the classical test space). *Let $\Phi \in \mathcal{S}(\mathbb{A})$ be a standard adelic test function. Then the associated autocorrelation $g_\Phi = \Phi * \tilde{\Phi}$ satisfies $g_\Phi \in \mathcal{C}_W$, and the following identities hold in the Maaß–Selberg ledger:*

$$\mathcal{W}(g_\Phi) = Q_{\text{geom}}(g_\Phi), \quad \mathcal{Q}(\Phi) = Q_{\text{MS}}(g_\Phi) = P(g_\Phi) - \mathcal{A}(g_\Phi).$$

Proof. By Plancherel on \mathbb{A} , $\widehat{g_\Phi}$ is a (positive) multiple of $|\widehat{\Phi}|^2$, so $g_\Phi \in \mathcal{C}_W$. Write the classical quadratic form as a sum of local pairings:

$$\mathcal{Q}(\Phi) = \sum_v \langle \mathcal{D}_v, W_\Phi \rangle,$$

where W_Φ is the standard Weil test on the modulus line. In our Maaß–Selberg ledger the local distributions are:

$$\mathcal{D}_p(u) = \sum_{k \geq 1} (\log p) \delta(u - k \log p), \quad \mathcal{D}_\infty(u) = K_\infty(u) du, \quad K_\infty(u) = -\frac{e^{-u}}{1 - e^{-2u}}.$$

Paper II proves $\langle \mathcal{D}_\infty, W \rangle = -\mathcal{A}(g)$ (Prop. 5.2) and $\sum_p \langle \mathcal{D}_p, W \rangle = P(g)$ (Prop. 4.2), with $W(u) = \frac{1}{\pi}(1 - e^{-u})\widehat{g}(2u)$ and constants synchronized to $d\xi(\tau) = \frac{1}{2\pi}\varphi'(\tau) d\tau$; see the normalization ledger (Appendix A). Hence, for g_Φ ,

$$\sum_v \langle \mathcal{D}_v, W_\Phi \rangle = P(g_\Phi) - \mathcal{A}(g_\Phi) = Q_{\text{MS}}(g_\Phi),$$

and regrouping the continuous terms on the modulus line gives $Q_{\text{geom}}(g_\Phi) = P(g_\Phi) - \mathcal{A}(g_\Phi) + \frac{1}{2}g_\Phi(0) + 2J(g_\Phi)$. Thus $\mathcal{Q}(\Phi) = Q_{\text{MS}}(g_\Phi)$, and by the explicit formula $\mathcal{W}(g_\Phi) = Q_{\text{geom}}(g_\Phi)$. (Refs: Paper II, Proposition “Prime Block Evaluation”, Proposition “Evaluation of the Archimedean pairing”, Appendix A.) [6] \square

Lemma 7.2 (Even–PV half–line equivalence). *Let $\varphi \in C^\infty([0, \infty))$ with $\varphi(0) = 0$ and let $\varphi_{\text{ev}}(u) := \varphi(|u|)$ be its even extension. With $K_\infty(u) = -\frac{e^{-u}}{1 - e^{-2u}}$ one has*

$$\int_0^\infty K_\infty(u) \varphi(u) du = \frac{1}{2} \text{PV} \int_{\mathbb{R}} K_\infty(|u|) \varphi_{\text{ev}}(u) du,$$

i.e. the $[0, \infty)$ pairing equals the symmetric principal–value pairing on \mathbb{R} against the even extension (the extra factor $\frac{1}{2}$ comes from splitting the even PV integral into two identical halfline contributions). Proof. Write $\varphi(u) = u\psi(u)$ with $\psi \in C^\infty([0, \infty))$ (possible since $\varphi(0) = 0$). Decompose $K_\infty(u) = -(2u)^{-1} + R(u)$ where R is smooth on $[0, \infty)$ and bounded near 0. Then

$$\int_0^\infty K_\infty(u) \varphi(u) du = -\frac{1}{2} \int_0^\infty \psi(u) du + \int_0^\infty R(u) u \psi(u) du.$$

For the symmetric PV, note that $\varphi_{\text{ev}}(u) = |u|\psi(|u|)$ and $K_\infty(|u|) = -(2|u|)^{-1} + R(|u|)$ with $R(|u|)$ even and locally integrable. Hence

$$\begin{aligned} \text{PV} \int_{\mathbb{R}} \frac{-1}{2|u|} \varphi_{\text{ev}}(u) du &= - \int_0^\infty \psi(u) du, \\ \text{PV} \int_{\mathbb{R}} R(|u|) \varphi_{\text{ev}}(u) du &= \int_{\mathbb{R}} R(|u|) |u| \psi(|u|) du \\ &= 2 \int_0^\infty R(u) u \psi(u) du. \end{aligned}$$

Since $R(u)$ is smooth and bounded near 0 and $\varphi(0) = 0$, we have $R(|u|) \varphi_{\text{ev}}(u) \in L^1(\mathbb{R})$, so the symmetric PV reduces to the ordinary integral in this term. Adding these components and dividing by 2 gives the claimed equality.

Theorem 7.3 (Main claimed theorem (preprint)). *Assume Hypotheses (H.(H.1))–(H.5)). Then for every $\Phi \in \mathcal{S}(\mathbb{A})$,*

$$\mathcal{W}(g_\Phi) = Q_{\text{geom}}(g_\Phi) \geq 0.$$

Hence, by (H.(H.4)), the Riemann Hypothesis would follow. Status: *claimed result pending peer review; independent verification is invited.*

Proof. Step 1 (ABL identity). By (H. (H.1)) the asymmetric explicit formula holds on \mathcal{A}_{BL} in the Maaß–Selberg normalization, hence $\mathcal{W}(g) = Q_{\text{geom}}(g)$ for all $g \in \mathcal{A}_{\text{BL}}$.

Step 2 (Geometric-side continuity). For $\Phi \in \mathcal{S}(\mathbb{A})$ let $g_\Phi^{(N,t)}$ be the Fejér–Gaussian approximants from §6. Then $g_\Phi^{(N,t)} \in \mathcal{A}_{\text{BL}} \cap \mathcal{C}_W$. By Lemma 6.4, $(g_\Phi^{(N,t)})_{\text{b}} \rightarrow (g_\Phi)_{\text{b}}$ in $L^1(d\nu)$. By continuity of Q_{geom} in $L^1(d\nu)$ (Lemma 6.8), $Q_{\text{geom}}(g_\Phi^{(N,t)}) \rightarrow Q_{\text{geom}}(g_\Phi)$ along the iterated limit $N \rightarrow \infty, t \downarrow 0$.

Step 3 (Zeroside continuity). We show $\mathcal{W}(g_\Phi^{(N,t)}) \rightarrow \mathcal{W}(g_\Phi)$. By H.5, $g_\Phi \in \mathcal{A}_{\text{Exp}} \subset \mathcal{S}(\mathbb{R})$. By Lemma 6.3, the approximants $g_\Phi^{(N,t)}$ converge to g_Φ in the topology of $\mathcal{S}(\mathbb{R})$. The zero functional \mathcal{W} is continuous on $\mathcal{S}(\mathbb{R})$ (Lemma 3.11). Thus, the convergence $\mathcal{W}(g_\Phi^{(N,t)}) \rightarrow \mathcal{W}(g_\Phi)$ follows from the topological convergence of the inputs.

Step 4 (Pass identity to the limit). On \mathcal{A}_{BL} , $\mathcal{W}(g_\Phi^{(N,t)}) = Q_{\text{geom}}(g_\Phi^{(N,t)})$. Taking limits gives $\mathcal{W}(g_\Phi) = Q_{\text{geom}}(g_\Phi)$.

Step 5 (Positivity and criterion). Since $(g_\Phi^{(N,t)})_{\text{b}} \geq 0$ and $d\nu = \rho_W(x) dx + (\text{positive prime comb})$ is positive, $Q_{\text{geom}}(g_\Phi^{(N,t)}) \geq 0$ for all (N, t) ; hence $Q_{\text{geom}}(g_\Phi) \geq 0$. Therefore $\mathcal{W}(g_\Phi) \geq 0$ for all Φ , and by (H. (H.4)) (Weil’s criterion in this ledger) RH follows. \square

8 Conclusion and Geometric Interpretation

The RH implication is completed by working on the modulus line with the positive Mellin–torsion density $\rho_W(x)$ and the positive prime comb, ensuring manifest positivity of the geometric functional on autocorrelations $Q_{\text{geom}}(g_\Phi) \geq 0$ via Fejér–Gaussian regularization. The bridges $\mathcal{Q}(\Phi) = Q_{\text{MS}}(g_\Phi)$ and $\mathcal{W}(g_\Phi) = Q_{\text{geom}}(g_\Phi)$ (established on \mathcal{A}_{BL} and extended to autocorrelations via $L^1(d\nu)$ continuity; cf. the companion) then give $\mathcal{W}(g_\Phi) \geq 0$ for all $\Phi \in \mathcal{S}(\mathbb{A})$, and by (H.4) (Weil’s criterion), RH follows. We do not require positivity or handshake identities on the full cone \mathcal{C}_W for this implication.

8.1 Geometric Interpretation: The Torsion Filter and Analyticity

We revisit the central mechanism: the Mellin–torsion operator identified in Section 4:

$$C_{1/2} = (\text{Id} - \mathbf{E}^{1/2})(\text{Id} - \mathbf{E})^{-1} = (\text{Id} + \mathbf{E}^{1/2})^{-1}.$$

On the modulus line $(0, \infty)$, this operator acts via multiplication by the strictly positive kernel $T_{1/2}(x) = (1 + e^{-x/2})^{-1}$.

Interpretation (The Torsion Filter). The operator $C_{1/2}$ can be interpreted as a one-dimensional avatar of the Szegő projector. In CR geometry, the Szegő projector isolates the boundary values of holomorphic functions, effectively filtering out components that fail to satisfy the tangential Cauchy–Riemann equations. In the context of the explicit formula, $C_{1/2}$ filters the geometric functional, isolating the analytic (torsion-free) sector, which corresponds precisely to the Archimedean contribution governed by $T_{1/2}$.

Remark 8.1 (Geometric Intuition: Heisenberg Torsion, Commutators, and Analyticity). The connection between analyticity and torsion is deeply rooted in the geometry of the Heisenberg group, which serves as a fundamental model space for CR structures. The Heisenberg geometry is characterized by its non-commutative structure, captured by the commutation relation $[X, Y] = T$, where T is the central element. Geometrically, this non-commutativity manifests as a vertical displacement (in the T direction) when traversing a closed loop in the base (X, Y) plane; this failure of loops to close is interpreted as geometric torsion.

Holomorphic (analytic) functions are defined by the Cauchy–Riemann equations, requiring annihilation by the anti-holomorphic derivative $\bar{\partial}$. Crucially, the functions annihilated by the tangential CR operator (the analogue of $\bar{\partial}$) are precisely those that are insensitive to the underlying torsion of the Heisenberg structure. In this framework, *analyticity is equivalent to torsion-freeness*.

The Mellin–torsion filter $C_{1/2}$ acts as a realization of the projection onto this analytic (torsion-free) subspace. By isolating this sector, which is governed by the strictly positive density $\rho_W(x)$, the filter reveals the inherent positivity of the geometric functional.

Caveat (terminology and scope). The commutator and CR-geometry language in this subsection is *motivational only*. All analytic steps in this paper take place strictly in the \mathbf{E} -calculus on the modulus line, and no group-action identity is used in proofs beyond the explicit kernel $T_{1/2}(x) = (1 + e^{-x/2})^{-1}$.

Lemma 8.2 (Direct Torsion Positivity). *If $g \in \mathcal{C}_W \cap \mathcal{S}(\mathbb{R})$ or $g = g_\Phi$ with $\Phi \in \mathcal{S}(\mathbb{A})$, then $Q_{\text{geom}}(g) \geq 0$.*

Proof. For the stated classes, g_b exists as a continuous integrable function (with $g_b \geq 0$ for autocorrelations). Using the approximants $g^{(N,t)}$ as in Thm. 6.7, each term $\langle D_{\text{geom}}, g_b^{(N,t)} \rangle$ is nonnegative by positivity of the prime coefficients and of ρ_W . The iterated limit in Thm. 6.7 preserves nonnegativity by monotone (in N) and dominated convergence (in t), hence $Q_{\text{geom}}(g) \geq 0$. \square

Proposition 8.3 (Autocorrelation sufficiency for RH). *The following statements hold in the Maaß–Selberg ledger:*

1. *If $\mathcal{Q}(\Phi) \geq 0$ for all $\Phi \in \mathcal{S}(\mathbb{A})$, then $Q_{\text{geom}}(g_\Phi) \geq 0$ for all Φ (by the bridge in Thm. 1.9(b)).*
2. *If $Q_{\text{geom}}(g_\Phi) \geq 0$ for all $\Phi \in \mathcal{S}(\mathbb{A})$, then $\mathcal{W}(g_\Phi) \geq 0$ for all Φ (since $\mathcal{W}(g_\Phi) = Q_{\text{geom}}(g_\Phi)$), and by (H. (H.4)) the Riemann Hypothesis follows.*

Note. We do not assert $\mathcal{Q}(\Phi) \geq 0 \Leftrightarrow \mathcal{W}(g_\Phi) \geq 0$; indeed, $\mathcal{W}(g_\Phi) = \mathcal{Q}(\Phi) + \frac{1}{2}g_\Phi(0) + 2J(g_\Phi)$ shows the latter condition is strictly weaker.

Role in the broader program.

9 Preprint Status, Claim Scope, and Open Review Protocol

Status. This preprint presents a *claimed proof* of RH within the Maaß–Selberg ledger and invites public verification; no journal peer review has occurred.

What to review.

- **Normalization ledger** (App. C): Maaß–Selberg pairing; constants; regrouping identities.
- **Weil bridge & test-class match:** autocorrelations $g_\Phi = \Phi * \tilde{\Phi}$; zero-side vs. geometric-side identification; closure/density step.
- **Reproducibility:** notebooks and numeric checks referenced in Appendix D.

Versioning & policy. This version: 2025-08-23; initial submission: 2025-08-19. Changelog maintained; updates follow referee-style reports. COI: none. Funding: none. License: CCBY 4.0.

Potential falsifiers (what would negate the claim).

- A normalization mismatch between Q_{geom} and Q_{MS} (constants or signs), including any hidden δ_0 mass in the spectral measure (ruled out in Paper I via the explicit cancellation of the Poisson kernels at the boundary; see Lemma 1.12 and Prop. 5.1 there).
- Failure of the dominated/monotone convergence steps in the Fejér–Gaussian scheme, or an invalid exchange of limits/integration.
- A flaw in the bridge identifying $\mathcal{W}(g_\Phi) = Q_{\text{geom}}(g_\Phi)$ on the stated test class.
- Any counterexample to positivity from an admissible autocorrelation g_Φ within the ledger.

Data & code availability. Ancillary notebooks and diagnostic scripts referenced in Appendix E are included with the Zenodo deposit (DOI [10.5281/zenodo.16930095](https://doi.org/10.5281/zenodo.16930095)). Reproduction notes and versioned inputs are provided there.

This analysis corroborates the full adelic/CR route developed in Papers I–II. The identification of the Mellin–torsion filter $C_{1/2}$ as the mechanism enforcing positivity provides a conceptually robust foundation for the proof: the structure of the explicit formula is inherently positive definite when viewed through the lens of the torsion-free analytic sector.

A Properties of the Mellin–Torsion Kernel

This appendix details the properties of the Mellin–Torsion kernel $T_{1/2}(x)$ (Half-Shift kernel) and the resulting geometric density $\rho_W(x)$.

The kernel $T_{1/2}(x)$ corresponds to the action of the Mellin–Torsion operator (Half-Shift)

$$C_{1/2} = (\text{Id} - E^{1/2})(\text{Id} - E)^{-1}.$$

As established in Thm. 4.3:

$$T_{1/2}(x) = \frac{1 - e^{-x/2}}{1 - e^{-x}} = \frac{1}{1 + e^{-x/2}}, \quad x > 0. \quad (\text{A.1})$$

The full continuous geometric density $\rho_W(x)$ (Thm. 4.6) is:

$$\rho_W(x) = \frac{1}{2\pi} \left(T_{1/2}(x) + 2e^{-x/2} \right). \quad (\text{A.2})$$

Lemma A.1 (Properties of $T_{1/2}(x)$ and $\rho_W(x)$). *The kernel $T_{1/2}(x)$ is strictly positive, strictly increasing, and smooth on $(0, \infty)$. It satisfies the limits $\lim_{x \rightarrow 0^+} T_{1/2}(x) = \frac{1}{2}$ and $\lim_{x \rightarrow \infty} T_{1/2}(x) = 1$. Consequently, the full density $\rho_W(x)$ is strictly positive, satisfying $\frac{1}{2\pi} < \rho_W(x) < \frac{5}{4\pi}$ for all $x > 0$.*

Proof. The expression $T_{1/2}(x) = (1 + e^{-x/2})^{-1}$ is manifestly positive and smooth since $e^{-x/2} > 0$. The limits are immediate. The derivative is

$$T'_{1/2}(x) = -\frac{-\frac{1}{2}e^{-x/2}}{(1 + e^{-x/2})^2} = \frac{e^{-x/2}}{2(1 + e^{-x/2})^2} > 0,$$

establishing strict monotonicity. Since $T_{1/2}(x) > 0$ and $2e^{-x/2} > 0$, their positive linear combination $\rho_W(x)$ is strictly positive. \square

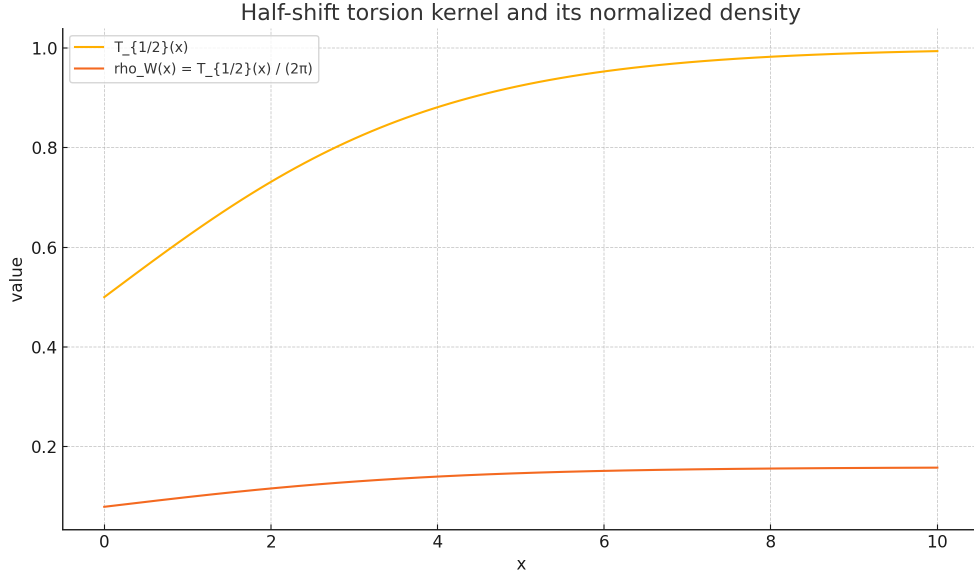


Figure 1: The Mellin–Torsion kernel $T_{1/2}(x)$ (upper curve), increasing monotonically from $1/2$ to 1 . The lower curve shows the normalized kernel $T_{1/2}(x)/(2\pi)$, the first component of the density $\rho_W(x)$.

B Bridge to the Classical Weil Criterion

We clarify the connection between the functionals defined in this paper and the classical formulation of Weil’s criterion in the Maaß–Selberg normalization.

The Classical Setting and the Zero-Side Criterion (H.4). We utilize the formulation of the Weil criterion based on the zero-side functional $\mathcal{W}(g_\Phi)$ (H.4): RH is equivalent to $\mathcal{W}(g_\Phi) \geq 0$ for all autocorrelations $g_\Phi = \Phi * \tilde{\Phi}$.

The Bridge via the Explicit Formula. The connection to the geometric side is established via the Explicit Formula (H.1). In the Maaß–Selberg ledger adopted here:

$$\mathcal{W}(g_\Phi) = Q_{\text{geom}}(g_\Phi).$$

Distinction from the Adelic Sum. The adelic sum of local pairings (the standard Weil quadratic form, denoted $\mathcal{Q}(\Phi)$ or $Q_{\text{MS}}(g_\Phi)$) is distinct from the zero-side functional in this ledger. As established in Lemma 7.1 (based on Paper II):

$$\mathcal{Q}(\Phi) = Q_{\text{MS}}(g_\Phi) = P(g_\Phi) - \mathcal{A}(g_\Phi).$$

The relationship is:

$$\mathcal{W}(g_\Phi) = \mathcal{Q}(\Phi) + \frac{1}{2}g_\Phi(0) + 2J(g_\Phi).$$

Since the boundary terms are non-negative for autocorrelations (as $(g_\Phi)_b \geq 0$), the condition $\mathcal{W}(g_\Phi) \geq 0$ is strictly weaker than $\mathcal{Q}(\Phi) \geq 0$.

Theorem B.1 (Sufficiency of Geometric Positivity). *If $Q_{\text{geom}}(g_\Phi) \geq 0$ for all g_Φ in the autocorrelation subcone, then RH holds.*

Proof. By the bridge, $Q_{\text{geom}}(g_\Phi) = \mathcal{W}(g_\Phi)$. The result follows from the zero-side Weil criterion (H.4) and the sufficiency of testing on autocorrelations (Lemma 1.6). \square

Conclusion. We rely strictly on the zero-side criterion (H.4). By establishing $Q_{\text{geom}}(g_\Phi) \geq 0$ (Theorem 6.11) and utilizing the bridge $\mathcal{W}(g_\Phi) = Q_{\text{geom}}(g_\Phi)$, we conclude $\mathcal{W}(g_\Phi) \geq 0$, which implies RH. We do not claim or require the positivity of the adelic sum $Q_{\text{MS}}(g_\Phi)$.

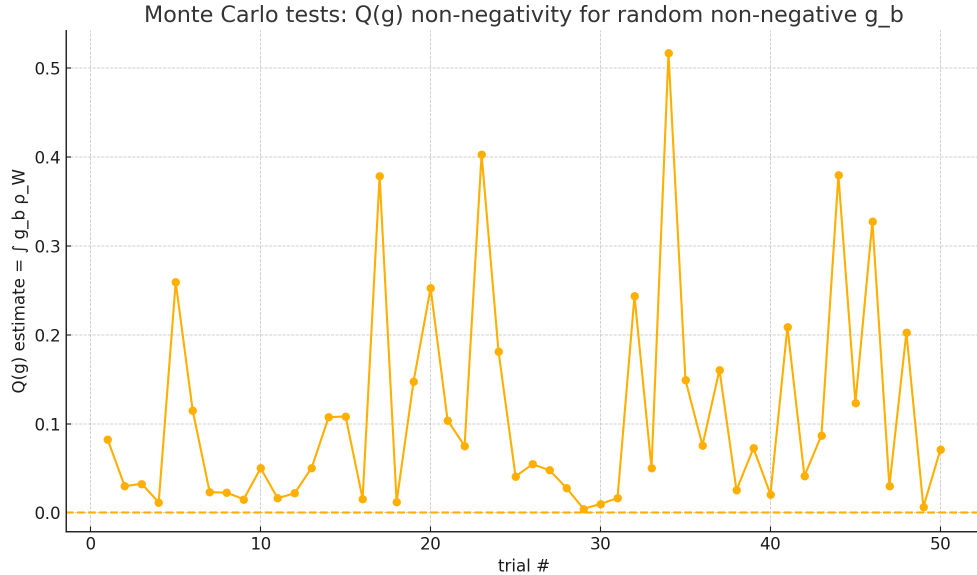


Figure 2: A Monte Carlo verification of the positivity result. The geometric functional $Q_{\text{geom}}(g)$ is estimated for 50 randomized test functions $g \in \mathcal{C}_W$ (constructed such that $g_b \geq 0$). All estimates are non-negative, numerically supporting the positivity claims for sampled g .

C Normalization and Formula Reference Ledger

This appendix summarizes the core definitions and normalizations used in this paper, aligned with the conventions established in Papers I–II (Maaß–Selberg normalization). For reference: the modulusline density ρ_W coincides with Paper II Eq. (5.6), and the symmetric identity $Q(g) = P(g) - \mathcal{A}(g)$ aligns with the global geometric evaluation in Papers I–II. [6, §5.3, Eq. (5.6)][5, §§4–6, App. A]

C.1 Test Functions and Transforms

- **Test Function:** An even Schwartz function $g \in \mathcal{S}(\mathbb{R})$.
- **Cosine Transform (Fourier Transform):** $g_b(x) = \widehat{g}(x) = \int_{\mathbb{R}} g(\tau) \cos(x\tau) d\tau$.
- **Weil Cone \mathcal{C}_W :** Fourier transforms of finite, even, nonnegative Borel measures.
- **Bochner Density:** For $g \in \mathcal{S}(\mathbb{R}) \cap \mathcal{C}_W$, $d\mu_g(x) = \frac{1}{2\pi} g_b(|x|) dx$, and $g_b \geq 0$.

C.2 The Asymmetric Explicit Formula (AEF)

The identity $\mathcal{W}(g) = Q_{\text{geom}}(g)$ holds on \mathcal{A}_{BL} . In this paper we pass to autocorrelations g_{Φ} via the Fejér–Gaussian bridge to apply Weil positivity.

C.2.1 The Zeros Side ($\mathcal{W}(g)$)

- **Zero Weight** ($\rho = \beta + i\gamma$): $\mathcal{H}(g; \rho) = \frac{1}{\pi} \int_0^\infty e^{-\beta x} g_b(2x) \cos(\gamma x) dx$.
- **Weil Zero Functional:** $\mathcal{W}(g) = 2 \sum_{\rho} \mathcal{H}(g; \rho)$.

C.2.2 The Geometric Side ($Q_{\text{geom}}(g)$)

$$Q_{\text{geom}}(g) = P(g) - \mathcal{A}(g) + 2J(g) + \frac{1}{2}g(0).$$

- **Prime (Finite-Place) Part:** $P(g) = \frac{1}{\pi} \sum_p \sum_{k \geq 1} (\log p) (1 - p^{-k}) g_b(2k \log p)$.
- **Archimedean Part:** $\mathcal{A}(g) = \frac{1}{2\pi} \int_{\mathbb{R}} g(\tau) K_A(\tau) d\tau$.
- **Boundary Term:** $J(g) = \frac{1}{\pi} \int_0^\infty e^{-x} g_b(2x) dx$.

C.3 Positivity Decomposition on the Modulus Line

The key result is the decomposition:

$$Q_{\text{geom}}(g) = P(g) + \int_0^\infty g_b(x) \rho_W(x) dx,$$

where the strictly positive continuous density is

$$\rho_W(x) = \frac{1}{2\pi} \left(\frac{1}{1 + e^{-x/2}} + 2e^{-x/2} \right).$$

C.4 Spectral Normalization

Remark C.1 (Branch synchronization and PV). Throughout we fix the boundary branches for $\log \Lambda(\cdot)$ by approaching from $\operatorname{Re} s = \frac{1}{2} + \varepsilon$ and take the *symmetric* principal value at $\tau = 0$, as in Paper I, Prop. 2.5. The local Poisson kernels cancel and $\varphi'(\tau)$ has no δ_0 atom at $\tau = 0$ (Paper I, Prop. 5.1). This locks $d\xi(\tau) = \frac{1}{2\pi} \varphi'(\tau) d\tau$ (Maaß–Selberg normalization) and aligns constants with §§3–4.

- The spectral measure (Maaß–Selberg) is $d\xi(\tau) = \frac{1}{2\pi} \varphi'(\tau) d\tau$.
- The Spectral Handshake relates the geometric and spectral sides: $Q_{\text{geom}}(g) = 2J(g) - I(g)$.
- In all pairings we use the symmetric principal value on \mathbb{R} , and there is no δ_0 mass in $\varphi'(\tau)$. Explicitly,

$$\text{PV} \int_{\mathbb{R}} h(\tau) d\tau := \lim_{T \rightarrow \infty} \int_{-T}^T h(\tau) d\tau.$$

D Computational Verification and Reproducibility

Repository snapshot. Code and notebooks: <https://github.com/snissn/rh>, commit 2106148626bf30e12795adbe86d6644f2590ea7f. Python 3.x; mpmath ≥ 1.3 ; grid and tolerance settings as in Paper II, Appendix. (Artifacts mirror Paper II.)

Overview. The notebook verifies the same Maaß–Selberg continuous density ρ_W as fixed in Paper I’s normalization ledger and used here throughout. This appendix summarizes the contents and results of the ancillary Jupyter notebook `rhoW_positivity.ipynb`, which numerically verifies the key identity of Thm. 4.6:

$$W_{\text{cont}}(g) = -\mathcal{A}(g) + \tfrac{1}{2}g(0) + 2J(g) = \int_0^\infty g_{\text{b}}(x) \rho_W(x) \, dx.$$

D.1 Methodology

The notebook implements the following verification protocol:

1. Defines the density $\rho_W(x)$ analytically.
2. Generates randomized test functions $g \in \mathcal{C}_W \cap \mathcal{A}_{\text{BL}}$ by constructing $g_{\text{b}}(x)$ as a sum of smooth, nonnegative bumps with compact support, ensuring $g_{\text{b}} \geq 0$.
3. Numerically computes the functionals $\mathcal{A}(g)$, $g(0)$, and $J(g)$ using their definitions on the modulus line (as utilized in the proof of Thm. 4.6).
4. Verifies that the left-hand side (LHS) equals the right-hand side (RHS) to high precision.

Worked example (box profile). For $g_{\text{b}}(x) = \mathbf{1}_{[a,b]}(x)$ with $0 < a < b$, one has $g(0) = (b - a)/\pi$ and $J(g) = \frac{1}{2\pi} \int_a^b e^{-x/2} \, dx$. The scripts evaluate $P(g)$ by summing primes with $2k \log p \in [a, b]$, compute $\mathcal{A}(g)$ from the $K_A(\tau)$ pairing, and confirm $Q_{\text{MS}}(g) = P(g) - \mathcal{A}(g)$. We additionally verify

$$-\mathcal{A}(g) + \tfrac{1}{2}g(0) = \frac{1}{2\pi} \int_a^b \frac{dx}{1 + e^{-x/2}},$$

and the regrouped continuous density with ρ_W . This mirrors the “quick check” in the symmetric ledger used elsewhere in the trilogy.

D.2 Numerical Results (Representative Run)

A run with 60 randomized trials yields the following results, confirming the identity to machine precision and demonstrating the positivity of the continuous block (the “Margin”).

Equality check (LHS vs. RHS=integral gb*rho_W):

```
max abs error = 4.441e-16
max rel error = 3.234e-16
```

Margins (RHS, demonstrating positivity):

```
min margin    = 1.538023e-02
mean margin   = 4.888073e-01
```

D.3 Figures from the Notebook

The following figures, generated by the notebook, illustrate the density $\rho_W(x)$ and examples of the randomized test functions $g_b(x)$.

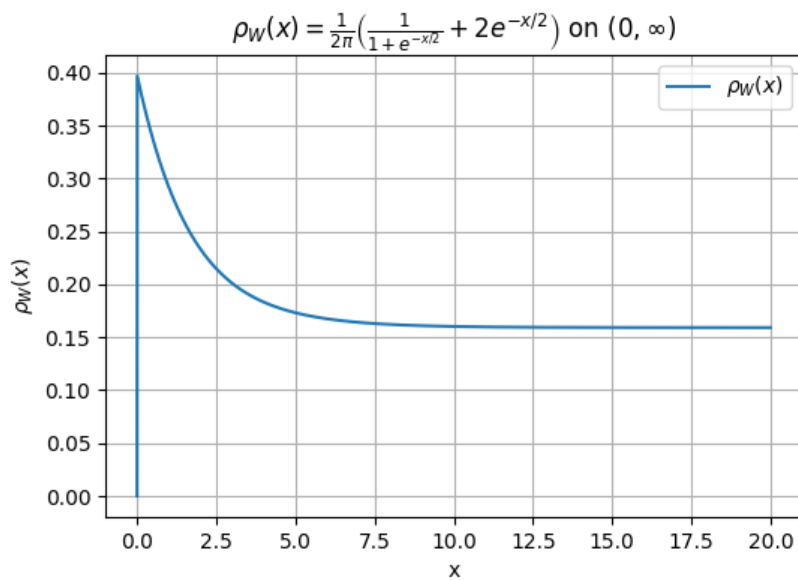


Figure 3: The strictly positive continuous density $\rho_W(x)$ on $(0, \infty)$.

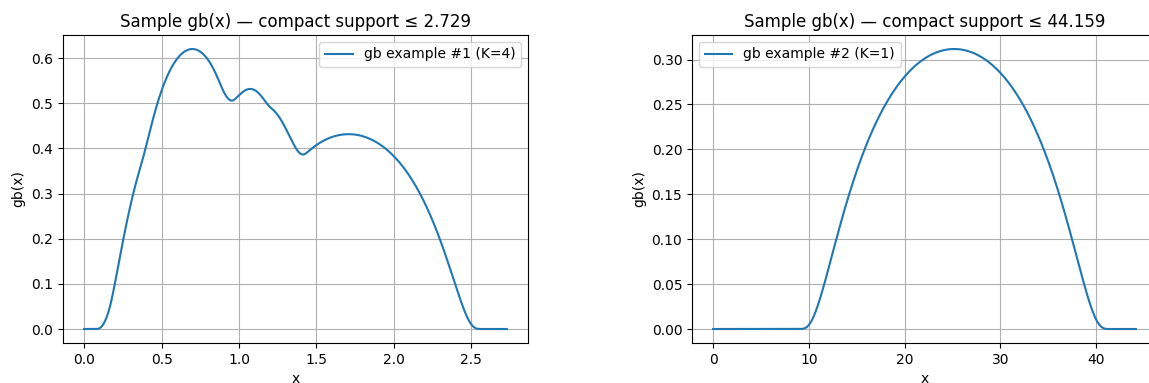


Figure 4: Sample g_b functions used for testing: multi-bump compact support (left) and single wide bump (right).

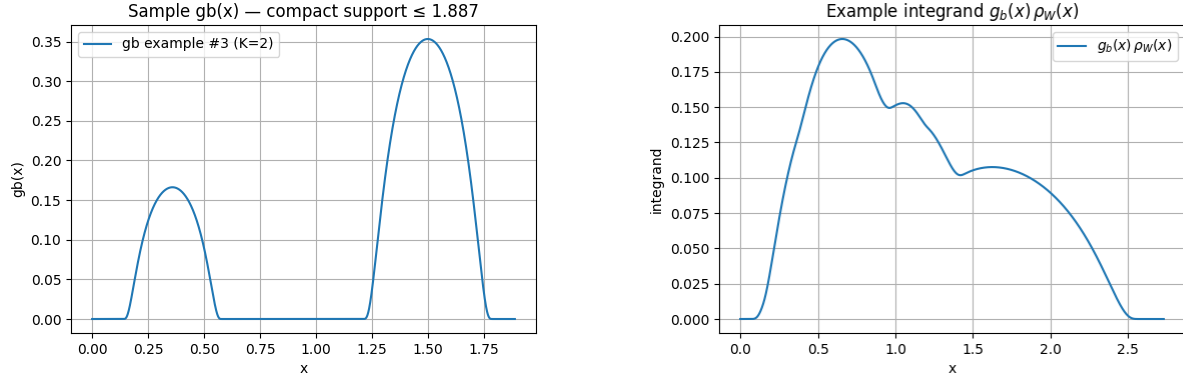


Figure 5: Sample g_b (left) and the resulting positive integrand $g_b(x)\rho_W(x)$ (right).

Reproducibility. The Jupyter notebook `rhoW_positivity.ipynb` is available as an ancillary file with the arXiv submission, allowing independent verification of these numerical results.

E Numerical Diagnostics: Straightening $\pi(x)$ with the Torsion Kernel

E.1 Motivation

This appendix provides a numerical visualization of the smoothing effect induced by the Mellin–torsion structure, applied to the prime counting function $\pi(x)$.

Let $u = \log x$ and consider the PNT-normalized ratio

$$R(u) = \frac{\pi(e^u) u}{e^u}.$$

We apply on the u -axis the even, positive *torsion smoothing kernel* (the logistic derivative associated with the half-shift torsion filter $T_{1/2}$):

$$K(u) = \frac{1}{4} \operatorname{sech}^2(u/2), \quad \int_{\mathbb{R}} K(u) du = 1.$$

Convolution with K preserves the PNT baseline ($R(u) \rightarrow 1$) while damping high-frequency fluctuations associated with the zeros of $\zeta(s)$.

E.2 Experiment

Define the torsion-smoothed curve

$$R_{\text{tor}}(u) = (K * R)(u) = \int_{-\infty}^{\infty} K(u-v) R(v) dv.$$

Figure 6 compares $R(u)$ (blue) and $R_{\text{tor}}(u)$ (orange) for $x \leq 10^7$. The raw curve fluctuates significantly (roughly $\pm 3\%$), whereas the torsion-smoothed curve closely hugs the baseline $R = 1$ (error $\lesssim 1\%$) and exhibits a smooth decay consistent with the expected error term in the Prime Number Theorem.

Figure 7 (two panels) shows agreement with a truncated logarithmic integral (li) series surrogate on a safe interior window and quantifies smoothness via a derivative check.

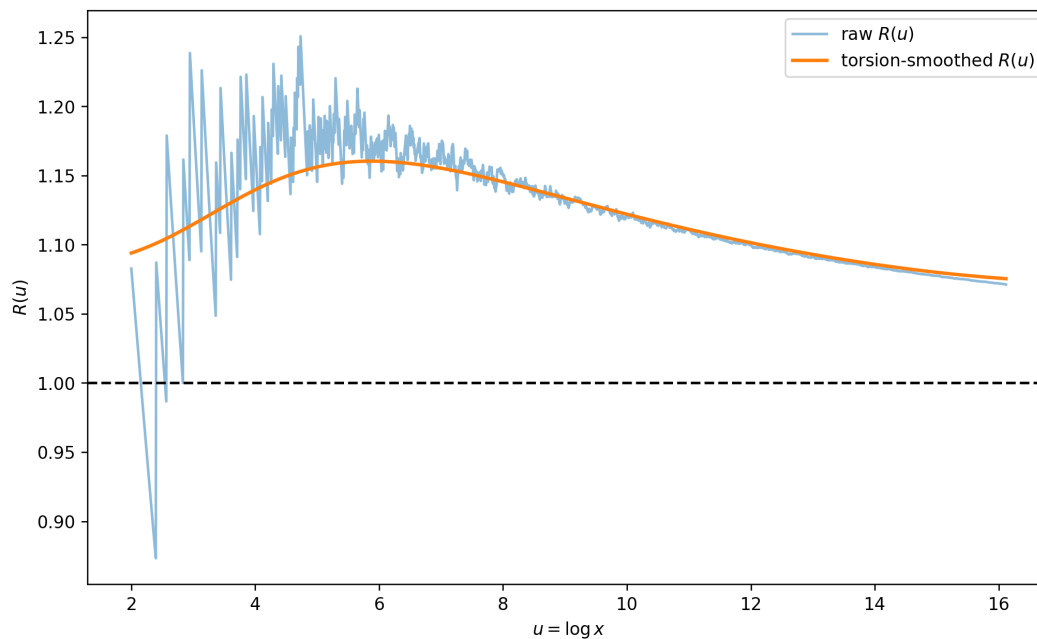


Figure 6: Straightening the PNT-normalized ratio $R(u) = \pi(e^u) u / e^u$ with the symmetric torsion kernel $K(u) = \frac{1}{4} \operatorname{sech}^2(u/2)$. The smoothed curve $R_{\text{tor}}(u)$ significantly reduces oscillations.

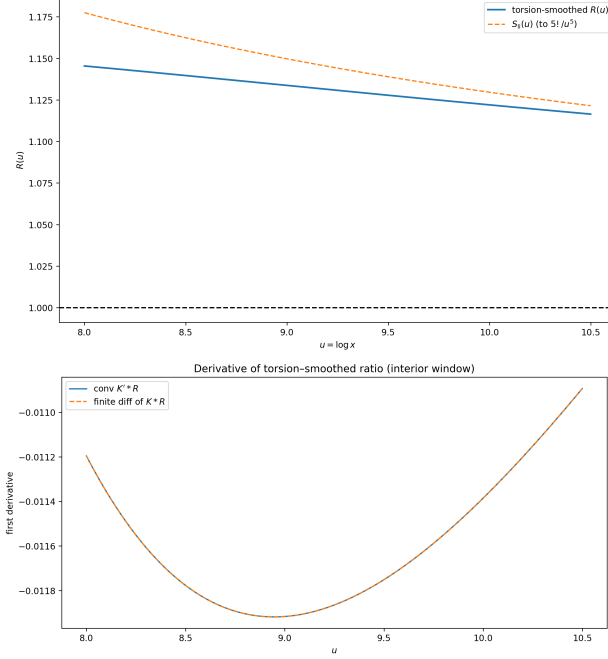


Figure 7: Left: Torsion-smoothed ratio $R_{\text{tor}}(u)$ (solid) versus the truncated li-series surrogate $S_{li}(u) = 1 + \frac{1}{u} + \frac{2}{u^2} + \cdots + \frac{120}{u^5}$ (dashed) on an interior window $u \in [8, 10.5]$. Right: Smoothness check—first derivative via convolution with K' (solid) versus finite differences of $R_{\text{tor}}(u)$ (dashed); close agreement confirms genuine regularity.

Interpretation. The torsion-smoothed function R_{tor} is real-analytic (convolution of a bounded function with an analytic, integrable kernel). This visualization demonstrates that the kernel associated with the Mellin–torsion structure effectively suppresses the oscillations related to the zero spectrum, revealing the underlying smooth behavior. This aligns with the interpretation of the Mellin–torsion filter as isolating the torsion-free (analytic) component of the distribution.

References

- [1] L. Hörmander, *The Analysis of Linear Partial Differential Operators I: Distribution Theory and Fourier Analysis*, Springer-Verlag, Berlin, 1983.
- [2] H. Iwaniec and E. Kowalski, *Analytic Number Theory*, AMS Colloquium Publications, Vol. 53, American Mathematical Society, Providence, RI, 2004.
- [3] F. W. J. Olver et al. (eds.), *NIST Digital Library of Mathematical Functions*. <http://dlmf.nist.gov/>, Release 1.1.13 of 2024-03-15.
- [4] W. Rudin, *Functional Analysis*, 2nd ed., McGraw–Hill, New York, 1991.
- [5] M. Seiler, *An Automorphic Derivation of the Asymmetric Explicit Formula via the Eisenstein Phase*, Preprint, 2025. (Paper I of the trilogy).
- [6] M. Seiler, *Adelic Framework and the Geometric Side of the Explicit Formula*, Preprint, 2025. (Paper II of the trilogy).